An-Najah National University

Faculty of Graduate Studies

MODIFICATION OF THE PROPERTIES OF CADIMIUM SELENIDE THIN FILMS IN PHOTOVOLTAIC SOLAR CELLS

By:

Huda Solaiman Mohamad Sabri, M.Sc. Physics student

Supervisors:

Dr. Subhi K. Salih, Ph.D.

And

Professor Hikmat S. Hilal, Ph.D.

Submitted in Partial Fulfillment of the Requirements for the Degree of Master of Science in PHYSICS, Faculty of Graduate Studies, at An-Najah National University, Nablus, Palestine.

2009

MODIFICATION OF THE PROPERTIES OF CADMIUM SELENIDE THIN FILMS IN PHOTOVOLTAIC SOLAR CELLS

By:

Huda Solaiman Mohamad Sabri

This thesis was defended successfully on 5/7/2009, and approved by:

Committee Members	**Signature**
1. Dr. Subhi Salih (Supervisor)	**……...**
2. Prof. Hikmat Hilal (Co-Supervisor)	**……**
3. Dr. Iyad Saadeddin (Internal Examiner)	**……**
4. Dr. Ayman Al Haj Daoud (External Examiner)	**……..**

Biographical Sketch

Huda S. M. Sabri, was born in Qalqelia. In 1981 she graduated from Qalqelia Secondary School. In 1999 she graduated from An-Najah National University (Nablus- Palestine) with the degree of Bachelor of Science in Physics. In 2005 she enrolled in Graduate College at An-Najah National University, and she had been engaged in research under the supervision of Professor Hikmat S. Hilal and Dr. Subhi Salih.

Dedication

To my husband…….

To my sons…….

To everyone who wants to revolute and enrich

his / her knowledge……..

Acknowledgements

The author wishes to express her sincere appreciation to her supervisors Dr. Subhi K. Salih and Professor Hikmat S. Hilal for their guidance, help and encouragement throughout research work and writing up.

The author would likes to acknowledge the assistance of Dr. Iyad A. Saadeddin and Mr. Ahed Zyuod (Ph.D. student) of An-Najah National University.

I wish to express my appreciation to the patience and encouragements given to me by my husband.

Huda S. Sabri

Nablus-An-Najah N.University

إقرار

أنا الموقع أدناه مقدم الرسالة التي تحمل العنوان:

تحسين خواص أفلام سلينيد الكادميوم الرقيقة في خلايا تحويل الضوئي الكهربائي

MODIFICATION OF THE PROPERTIES OF CADIMIUM SELENIDE THIN FILMS IN PHOTOVOLTAIC SOLAR CELLS

اقر بأن ما هذه الرسالة ككل اشتملت عليه هذه الرسالة إنما هي نتاج جهدي الخاص، باستثناء ما تمت الإشارة إليه حيثما ورد، وان هذه الرسالة ككل، أو أي جزء منها لم يقدم من قبل لنيل أية درجة علمية أو بحث علمي أو بحثي لدى أية مؤسسة تعليمية أو بحثية أخرى.

Declaration

The work provided in this thesis, unless otherwise referenced, is the researcher's own work, and has not been submitted elsewhere for any other degree or qualification.

Student's name: **اسم الطالب:**

Signature: **التوقيع:**

Date: **التاريخ:**

List of Contents

List of Figures

List of Tables

XVIII

MODIFICATION OF THE PROPERTIES OF CADMIUM SELENIDE THIN FILMS IN PHOTOVOLTAIC SOLAR CELLS

By

Huda Solaiman Mohamad Sabri

Abstract

Polycrystalline cadmium selenide, CdSe, thin films were prepared by chemical bath deposition (CBD) technique. The films were deposited using cadmium chloride as a Cd^{+2} ion source, and sodium selenosulphite as a Se^{-2} ion source. Annealing the films in air for 10 minutes at 100 ^{0}C-350 ^{0}C affected the grain growth. The annealed films were returned to room temperature either by quenching or slow cooling. The energy band gap (E_g) decreased with increasing thicknesses and substrate temperatures. Value of E_g calculated from UV/visible absorption spectra ranged between 2 and 1.83 eV. The used film thickness was ~10μm. Annealing and rate of cooling that present the best photoluminescence (PL), photo and dark currents for the film electrodes are discussed here. Covering CdSe thin films with metalloporphyrine complex, embedded inside polymeric polysiloxane matrices, enhanced the electrode efficiency and stability. The deposited films were investigated by optical PL and UV absorption spectra.

Chapter One

INTRODUCTION

Many bi-products, such as CO_2, sulfur and nitrogen oxides may result in global warming and acid rain. So, it is time that the world slowly changes from using non-renewable energy to renewable energy. Renewable energy is derived from sources that are regenerative, such as solar energy. Recently, photovoltaic (PV) effects have been reported in structures consisting of nanocrystals forming junctions with organic semiconductor polymers. Successful PV effects in such cells have been reported for semiconductor nanocrystals (NC) including InP, CdSe, CdS, and PbS [1].

1.1 OBJECTIVES

The main objective of this work is to use simple techniques to enhance characteristics of CdSe thin films prepared by Chemical Bath Deposition (CBD) onto fluorine-doped tin oxide FTO/glass substrates. It is intended to enhance electronic absorption (EA) spectra and photoluminescence (PL) spectra. Moreover, enhancement of the efficiency and stability of CdSe thin films in light–to-current conversion processes is also intended as seen in I_{sc} and J-V plots. For these objectives, the following techniques will be experimented:

1- Preheating the sample of CdSe at different temperatures.

2- Precooling the sample of CdSe in different ways: by quenching and slow cooling.

3- Coating the CdSe thin film with metalloporphyrine ions MnP embedded inside a polysiloxane polymer matrix.

1.2 HYPOTHESIS

Annealing semiconductor thin films would enhance their characteristics in different applications, including photoelectrochemical cell (PEC) study. This is because annealing is assumed to enhance grain size and eliminate grain boundaries between them. Moreover, annealing should remove imperfections within the microcrystal of the thin film. On the other hand, slow cooling is assumed to yield more ordered micro-crystals than quenching. This is because slow cooling will allow metastable components to return to their origin, and remove cracks. Fast cooling may also help cure the crystals without prolonged exposure to high temperatures, thus yielding more uniform micro crystals. Covering CdSe thin films with polymeric matrices having electroactive species, such as metalloporphyrine is assumed to enhance its PEC characteristics. Firstly, the polymer matrix should protect the CdSe film. Secondly, the metalloporphyrine (Mn^{II}/Mn^{III})

P would behave as charge transfer catalyst across the solid/ liquid interface, thus enhance quick release of holes. This would enhance photocurrent and would enhance the semiconductor electrode stability.

1.3 Previous Studies

Cadmium selenide and cadmium telluride have been studied in PV cells constructed of single crystal semiconductor material in contact with electrolyte solutions [2]. CdSe showed an open-circuit voltage near 0.8V and power conversion efficiencies near 6% for 720-nm light [3]. Mono crystalline CdSe wafers have been used as PV devices [4]. Many workers reported PV solar cells of nanocrystals [5]. On the other hand, many other workers used thin films of CdSe on conducting glass [6]. The morphology of CdSe thin films prepared by CBD is strongly affected by the substrate used for the deposition. The different morphology on the micrometer scale leads to very different mechanical and optical properties of the films. The films grown on glass substrates are of very good mechanical and optical quality while the deposition on carbon-coated glass leads to the growth of films of quite poor mechanical durability [7]. UV–visible absorption spectroscopy of the as prepared nanoparticles shows the presence of direct transition with energy band gap of about 2.02 eV. Comparing to 1.74 eV, corresponding to its bulk value, a blue shift of about 0.28 eV is detected

which is understood as a quantum size effect, due to confinement of electron and hole in a small volume [8]. It is concluded that the deposition of CdSe at lower, temperatures results in smaller grain size and thickness than at higher deposition temperature. Due to the variation of grain size and thickness, the electrical resistivity increases and CdSe show `blue shift' of 0.5 eV [9]. The deposition of CdSe semiconductor films on commercially available microscope glass slides by CBD method is reported. At room temperature acceptable quality CdSe films were obtained above 24 hours. By increasing deposition time to 74 hours acceptable crystallinity, compact and homogeneous films with well defined, spherical and similar size grains, having a fine grain background, were obtained at the same bath conditions. At 60 °C the best films were obtained at 2 and 3 hours. The deposition was observed in a single cubic phase, while no peaks due to hexagonal phase were observed [10]. Cadmium selenide films have been deposited from ammonia-free bath using sodium citrate as a complex agent for cadmium ions in weak alkaline bath (pH < 9.0). The deposition has been carried out onto different substrates such as titanium, nickel, and ITO coated glass. The CdSe films showed hexagonal crystal structure irrespective of type of substrate. The CdSe films were photoactive [11]. The investigation of CdSe nanoparticles, prepared using two different

synthetic routes, showed similar crystallographic and optical properties. The reported photoluminescence line shapes and the dependence on excitation power and temperature are all indicative of a recombination between trapped electrons and holes, presumably located at surface sites [12]. Within a certain temperature range, the band gap absorption peak position (k in nm) of CdSe nanocrystals with a given particle size (D) can be expressed as a simple linear function of temperature (T in K): k = 0.1 T + C (D, 298 K) [13].

Highly ordered TiO2 nanotube films were fabricated by a simple anodic oxidization process. The TiO2 nanotubes can be converted into anatase phase by annealing in air. Attachment of CdSe quantum dots significantly extends the photo-response of the TiO2 nanotubes in the visible region [14-15].

1.4 Energy Band Gap:

If an electron acquires enough additional energy from an external source, it leaves the valence band (V.B.) and becomes a free electron in what is known as a conduction - band (C.B.), Figure(1.1). The difference in energy between the valence band upper edge and the conduction band lower edge is called the energy band gap E_g [16]. This is the minimum amount of

energy that a valence electron must have in order to jump from the valence band to the conduction band.

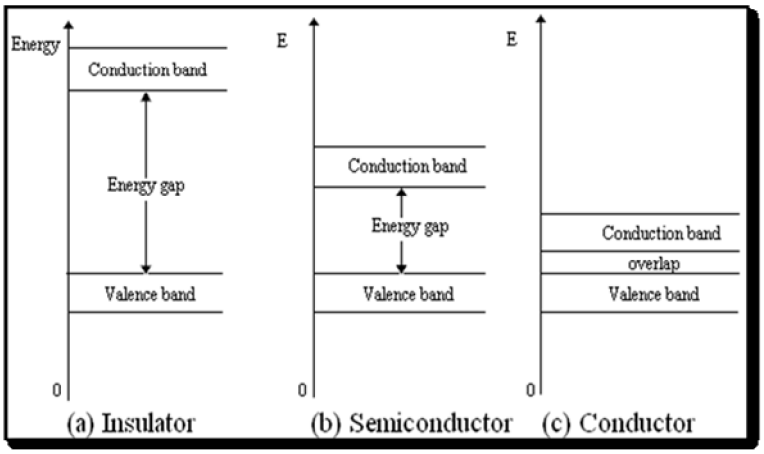

Figure (1.1): A schematic showing band structure for (a) insulators, (b) semiconductors and (c) conductors.

Materials are classified according to their E_g in to three types [17]. Insulators that have wide E_g Figure (1.1-a), semiconductors with E_g less than that for insulators Figure (1.1-b), and conductors with overlapping between the valence and conduction bands Figure (1.1-c).

1.5 Conduction in Semiconductors

An intrinsic (pure) silicon crystal at room temperature gains heat (thermal) energy from the surroundings, causing some valence electrons to gain sufficient energy to jump the gap from the valence band into the conduction band. The excited electron are thus free electrons, not bound to any atom but free to drift [18]. Free electrons are called ***conduction electrons($\bar{e}$)***. When an electron jumps to the conduction band, a vacancy is

left in the valence band. This vacancy is called a ***hole (h^+).*** Electron-hole recombination may or may not occur [19]. If recombination occurs energy is emitted. Otherwise, electron-hole separation occurs.

1.6 Electron and Hole Current

When a voltage is applied across a piece of intrinsic silicon, electrons, which are free to move randomly in the crystal structure, are now easily attracted toward the positive electrode. This movement is one type of current in a semiconductor material and is called ***electron current***. Another type of current occurs in the valence band, by hole immigration. Valence band electrons are tightly bound to their atoms and are not free to move randomly. Effectively, the holes move from one place to another across the valence band. This is called ***hole current*** [20].

1.7 The p-n Junction:

If we take a block of silicon and dope one side of it with a trivalent impurity and the other side with a pentavalent impurity, a boundary called the p-n junction is formed between the resulting p-type and n-type portions. The p-n junction is the feature that allows diodes, transistors, and other devices to work [21]. The pn junction is shown in Figure (1.2).

1.8 Formation of the Depletion Region:

Before the p-n junction is formed, there are as many electrons as protons in the n-type material making the material neutral in terms of net charge. The same is true for the p-type. When the p-n junction is formed, the n region loses free electrons as they diffuse across the junction. This creates a layer of positive charges (pentavalent ions) near the junction. As the electrons move across the junction, the p region loses holes. This creates a layer of negative charges (trivalent ions) near the junction. These two layers of positive and negative charges form the so- called ***depletion region*** [22].

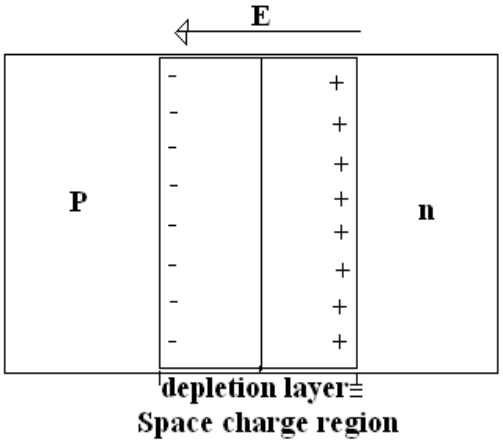

Figure (1.2): depletion layer which is the space charge region in pn structure.

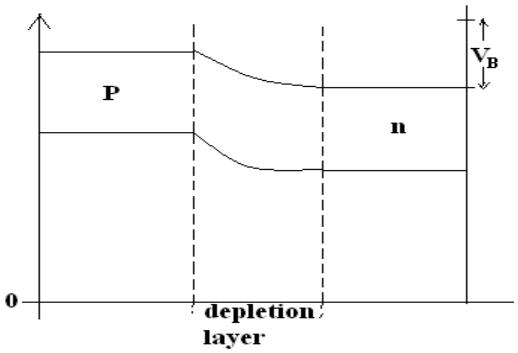

Figure (1.3): Potential barrier created due to depletion layer formation.

1.9 Barrier Potential (V_B):

In the depletion region there are many positive and negative charges on opposite sides of the p-n junction. The forces between the opposite charges form a "field of forces" called an ***electric field***. This electric field is a barrier to the free electrons in the n region, and energy is needed to move an electron through the electric field. That is, external energy must be applied to get the electrons to move across the barrier of the electric field in the depletion region [23]. This potential difference is called the ***barrier potential***. The most commonly known solar cell is configured as a large-area p-n junction made of silicon. The electric field, established across the p-n junction, creates a diode that promotes current to flow in only one direction across the junction. Electrons may pass from the n-type side into the p-type side, and holes may pass from the p-type side to the n-type side. This region where electrons have diffused across the junction is called the depletion region because it no longer contains any mobile charge carriers. It is also known as the "Space Charge Region" [24]. The depletion layer and space charge region are shown in Figures (1.2) and (1.3).

1.10 Techniques of Light-to-Electricity Conversion:

There are two types of strategies to convert light into electricity using semiconducting materials.

i) Photovoltaic Cells: (PV)

Photovoltaic energy is the conversion of sunlight into electricity through a photovoltaic (PV) cell, commonly called a ***solar cell***. The solar cell is the basic building block of solar voltaics. The cell can be considered as a two terminal device which conducts like a diode in the dark and generates photovoltage when charged by the sun. The basic unit generates a DC photo voltage of 0.5 to 1 volt [25]. The current is too small for most applications. So, the cells are connected together in series to generate output voltage of 12 volt in standard illumination conditions as shown in Figure (1.4).

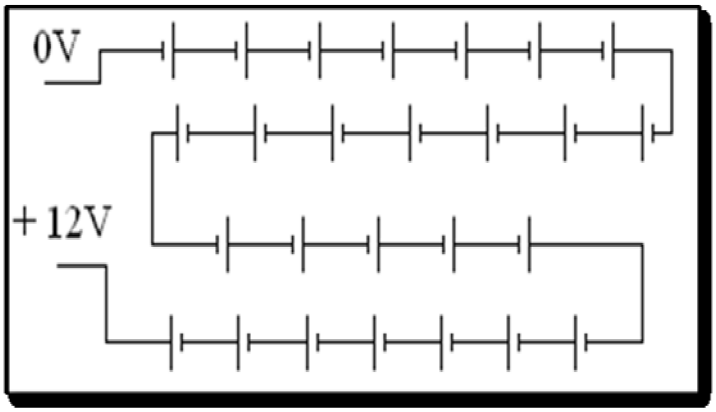

Figure (1.4): Solar batteries in series.

A battery is used to store charge generated during sunny periods as in Figure (1.5) [26].

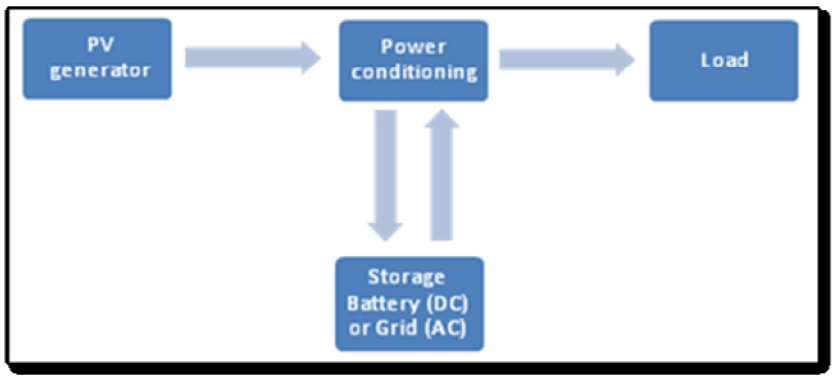

Figure (1.5): Storage of solar energy in photovoltaic cell.

When DC from photovoltaic cells is used for commercial applications or sold to electric utilities using the electric grid, it must be converted to alternating current (AC) using inverters, which are solid state devices that convert DC power to AC [27]. Solar power is pollution free during use. Production of wastes and emissions are manageable using existing pollution controls. Solar electricity can sometimes be more expensive than electricity generated by other sources. Solar electricity is not available at night and may be less available due to weather conditions. Solar cells produce DC which must be converted to AC when used in currently existing distribution grids. This incurs an energy loss of (4-12)% [28-30]. An equivalent circuit of ideal solar cell is shown in Figure (1.6).

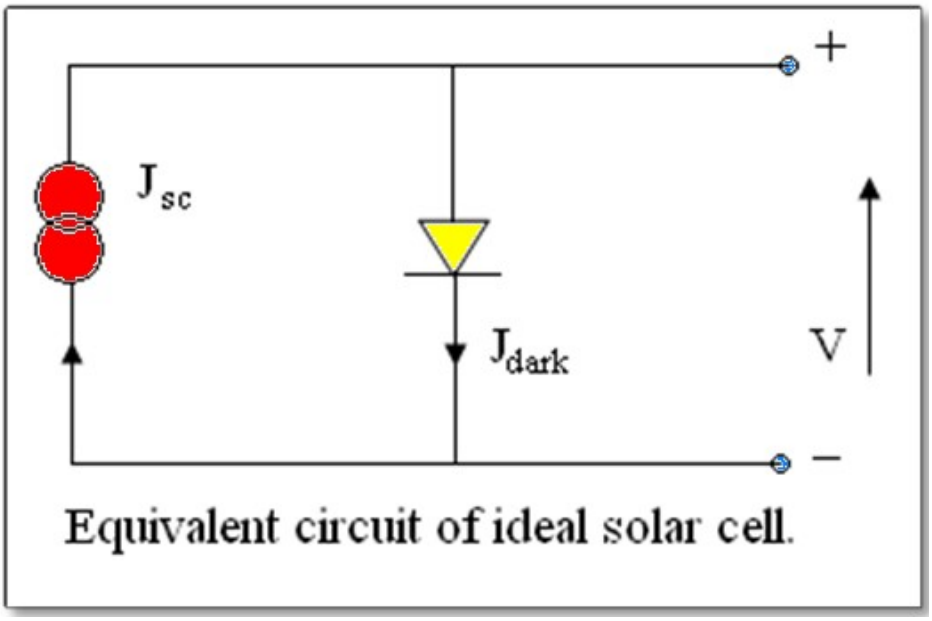

Figure (1.6): Equivalent circuit of ideal solar cell.

ii) Photoelectrochemical Cell (PEC):

a) The Semiconductor-Electrolyte Interface:

All phenomena associated with PEC systems are based on the formation of a semiconductor-electrolyte junction when an appropriate semiconductor is immersed in an appropriate electrolyte. The junction is characterized by the presence of a space charge layer (SCL) in the semiconductor adjacent to the interface with electrolyte. A space charge layer generally develops in a semiconductor upon contact and equilibrium with a second phase whenever the initial chemical potential of electrons is different for the two phases. For semiconductors, the chemical potential of electrons is given by the Fermi level (E_f) in the semiconductor. For liquid electrolytes, it is determined by the redox potential of the redox couples present in the

electrolyte; those redox potentials are also identified with the Fermi level of the electrolyte [31]. The energy level diagram for SC-electrolyte junction is shown in Figure (1.7).

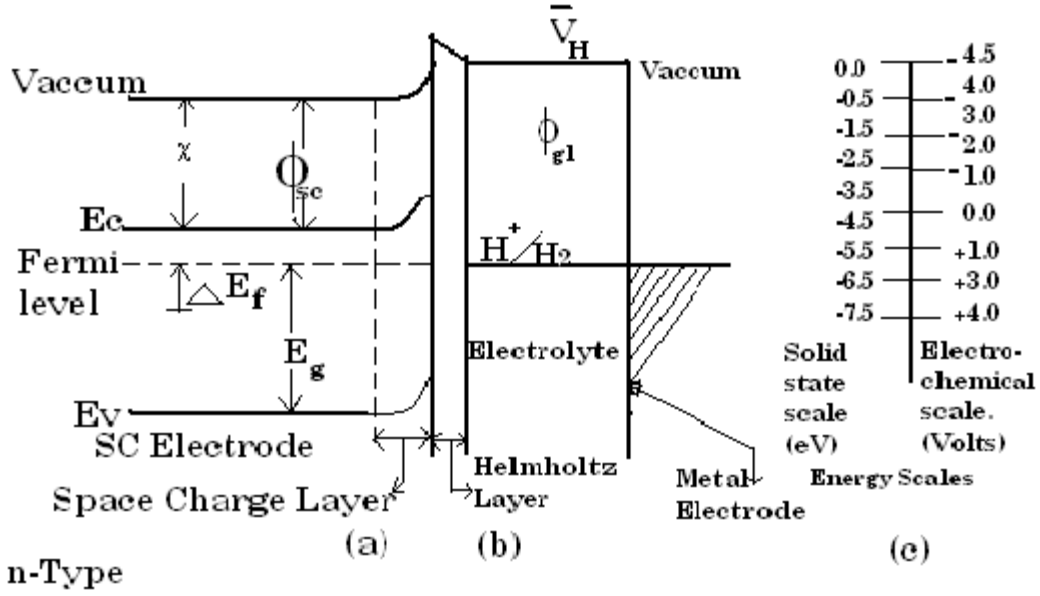

Figure (1.7): Energy level diagram for SC-electrolyte junction showing the relationship between the redox couple (H/H_2), the Helmholtz layer potential drop (V_H), and the SC band gap (E_g), electron affinity (χ), work function (Φ_{sc}), band bending (V_B), and the flat band potential (V_{fb}). The electrochemical and solid state energy scales are shown for comparison. Φ_{E1} is the electrolyte work function.

b) Principles of PEC Energy Conversion:

PEC systems are based on the formation of a SC/electrolyte junction when a SC is immersed in a suitable electrolyte solution. A depletion region or space charge layer (SCL) is formed as a result of n-type SC-electrolyte junction. For SC, the Fermi level (E_F) in the SC is determined by chemical potential of majority carriers (electrons). For electrolyte solutions, the redox couples determine the initial chemical potential. When n-type SC is

brought into contact with an electrolyte solution, the following energetics will be exhibited. Before equilibrium the E_F will remain above E_{redox}. Electrons will therefore flow down to E_{redox}. As a result, E_F will be lowered. The electrons flow will continue until the equilibrium is established. At equilibrium, E_F and E_{redox} will match up. Consider an n-type SC and a counter electrode in contact with the same electrolyte containing a redox couple. The two electrodes are externally connected to each other with a variable series load resistance R ($0 < R < \infty$); this type of PEC cell is called regenerative cell, as shown in Figure (1.4-a). At equilibrium the Fermi level of the SC and the redox potential of the solution are adjusted in the same level [32]. When the SC is illuminated the Fermi level of the SC will

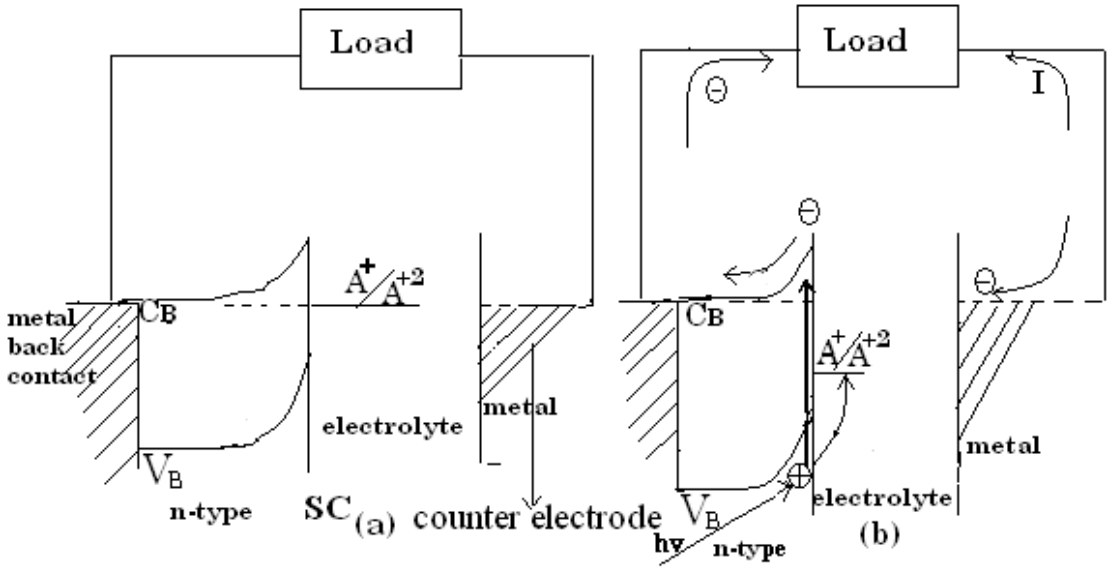

Figure (1.8): Energy level diagram regenerative cell at:

equilibrium and (b) during illumination.

rise. The counter electrode Fermi level will also rise, depending on the value of R. The rise of Fermi level depends on the rate of charge transfer at the metal counter electrode. At R = 0 the electrodes are short – circuited (sc) to each other, and they will have the same Fermi level. The excited electrons will move through R to the counter electrode and reduce the ions in the electrolyte as shown in Figure (1.4-b) [33].

1.11 Dark Current:

In the dark, at equilibrium, there exists a potential barrier between the surface and the bulk of the electrode. The band bending in both valence and conduction bands (V_B) represents this potential. Occurrence of dark current is due to electron transfer from the n-type SC conduction band to the electrolyte across the interface. To achieve this, a negative potential (ΔE) must be applied, to provide electrons with enough energy to overcome this barrier, consequently no SCL will appear (flat band) [34].

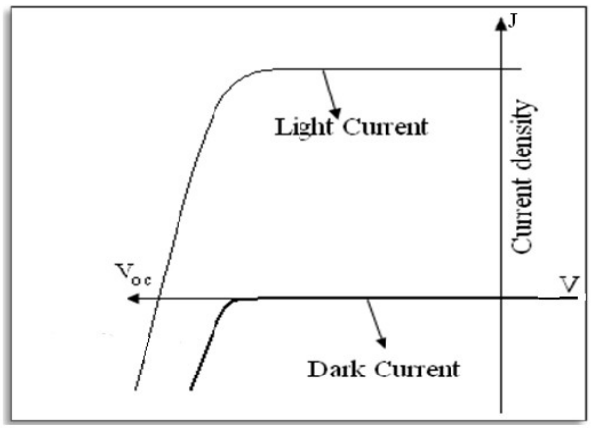

Figure (1.9): Dark and photo currents observed in an n- SC/electrolyte PEC cell.

1.12 Photo Current:

When light absorption generates population of excited holes and electrons, in n-type SC, the majority carrier concentration changes relatively little and the minority carrier concentration is greatly enhanced. Hence photocurrents are greatest when minority carriers dominate the electrode response. Photo generated minority carriers (holes) migrate across the SC –electrolyte interface, with an oxidizing power to oxidize a *red* form of the redox couple, and affect both photocurrent and photo potential:

$h^+ + red \longrightarrow ox^+$ [35-36].

As an initial approximation photo effect switches on as the wave length of the incident light (λ) decreases below the threshold wavelength (λ_g). With λ shorter than λ_g the electrode is relatively insensitive to light. A useful relation between λ_g and E_g [37] is : $\lambda_g = \frac{1240}{Eg}$

Where λ_g has units of nanometers, and E_g has units of (eV). The dependence of photocurrent and photo potential on excitation wavelength gives information about band gap energy and nature of optical transition (direct or indirect). Recombination is another important phenomenon of photo-effects in the PEC. Recombination can occur directly with the electron descending from the conduction band to the hole edge at the

valance band edge, or indirectly via intermediate energy levels (bulk or surface states) [38]. Recombination reduces the magnitude of photo effect, and consequently lowers the power and the efficiency of PEC cell. When n-type SC electrode is biased relatively positive of flat band $\mathbf{V_B}$ the dark currents are very low, due to blocking effect of the SCL. Upon the irradiation of the SC through the electrolyte with light (λ shorter than λ_g), large anodic photocurrents appear. These photocurrents arise from the flux of holes (minority carrier) arriving at the surface . The generated electron –hole pairs in the SCL are separated by the electric field in the SCL. Electron –hole pairs, generated beyond the SCL, depends on the energy distribution of the incident photons, the absorption coefficient of the SC, the diffusion distance of the excited holes and electrons, and the recombination rates [39]. As the applied potential approaches V_B the space charge layer thickness decreases. Recombination rates increase because the holes and electrons are no longer being separated by the electric field. The photocurrent drops sharply and merge with the dark current near $V_{B.}$ At applied potential equals negative of V_B, the electrode is no longer blocking , and the dark current increases dramatically, with small anodic photocurrent sometimes observed [40].

1.13 Perturbations of the Ideal Model of PEC Systems :

SC electrode behavior is not as ideal as discussed in the preceding section. A number of phenomena occur that add a complication to the ideal model

i) Corrosion :

Rapid change in the surface composition results when the SC crystal becomes in contact with the aqueous electrolytes. The photo- generated holes and electrons are generally characterized by strong oxidation and reduction potentials, respectively. Instead of being injected into the electrolyte to drive redox reactions they cause SC surface corrosion [41]. Generally an oxide layer forms and causes SC surface decomposition. The oxides include pH sensitivity of V_B electrode surface. When current flows across the solid –liquid interface, the surface can undergo further alteration. The most severe changes result when holes oxidizing equivalents arrive at the surface. Thus n-type SC's are particularly susceptible to photo-corrosion. Both soluble and insoluble products may be formed. The insoluble products build upon the surface, and may block current flow [42].

ii) Surface States:

In the usual model of charge transfer across SC/electrolyte interfaces, it is assumed that occurrence of this process is so energetic. As shown in Figure (1.6), electrons can only be exchanged between the SC and the electrolyte if the energy levels of the valance band overlap with the occupied energy levels of the electrolyte redox couple (anodic current flows by hole injection), or if the conduction band overlap with the empty energy levels of the electrolyte redox couple (cathodic current flows by electron injection) [43]. However experimental results show that the inverse is generally true. These results are generally explained by involving the existence of surface states. The surface states, or intermediate trapped charges, exist within the forbidden E_g of the SC [44]. These states result from different sources, including structural defects, metallic impurities, or bond breaking processing. Surface states are most effective when they are located energetically between the band edges at the surface. They mediate charge transfer of majority and minority carriers, control surface charge and band bending and catalyze recombination of photo generated charge carriers.

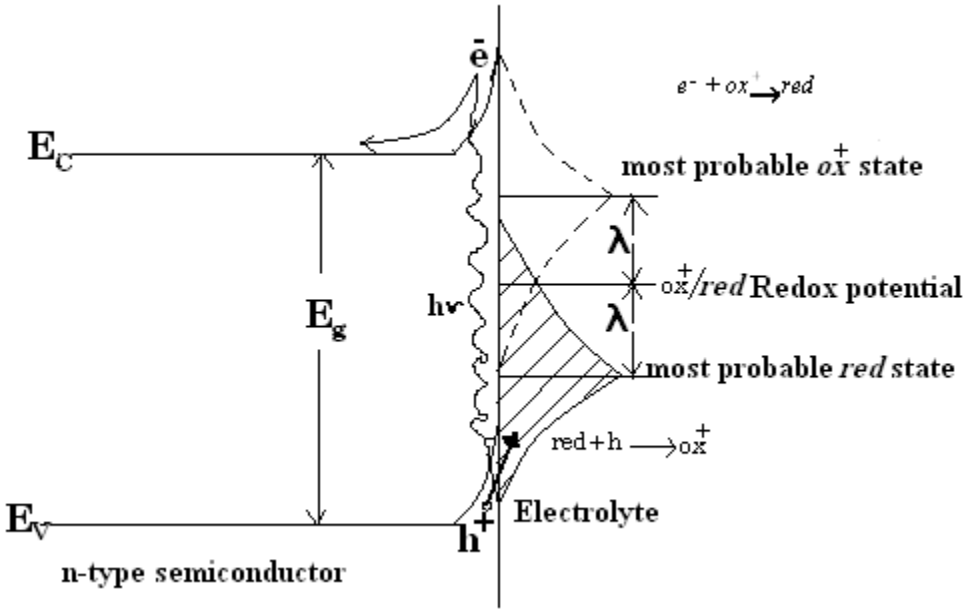

Figure (1.10): Isoenergetic charge transfer of hole from n-type SC to occupied state of electrolyte redox couple. Redox energy levels have a distribution due to solvent-ion interactions.

The existence of surface states lowers the resulting photocurrent density. Surface states may be classified as intrinsic or extrinsic [45]. Intrinsic states arise from the abrupt termination of the crystal lattice at the electrode surface. The dangling bonds in the crystal will dangle long in an electrolyte. The new chemical entity formed by reaction with a solution spieces may then behave as a surface state. Extrinsic states are created when a new phase is formed at the interface, or when the electroactive species (of the redox couple) adsorb to the electrode surface [46]. They are, in principle, removable when the surface is renewed. Consider an n-type SC in contact with an electrolyte containing an (ox) species, the standard potential for the reduction of (ox) is more positive than V_B Figure (1.7-a).

Surface states can provide an alternative path; the electrons tunnel through the SCL to the surface states and then transfer to the (ox) spieces. The holes in the valance band are captured by surface states in the band gap, which then oxidize the red molecules, Figure (1.7-b).

The surface states overlap more effectively with the higher red energy levels. The arrival of holes at the surface may create surface states [47].

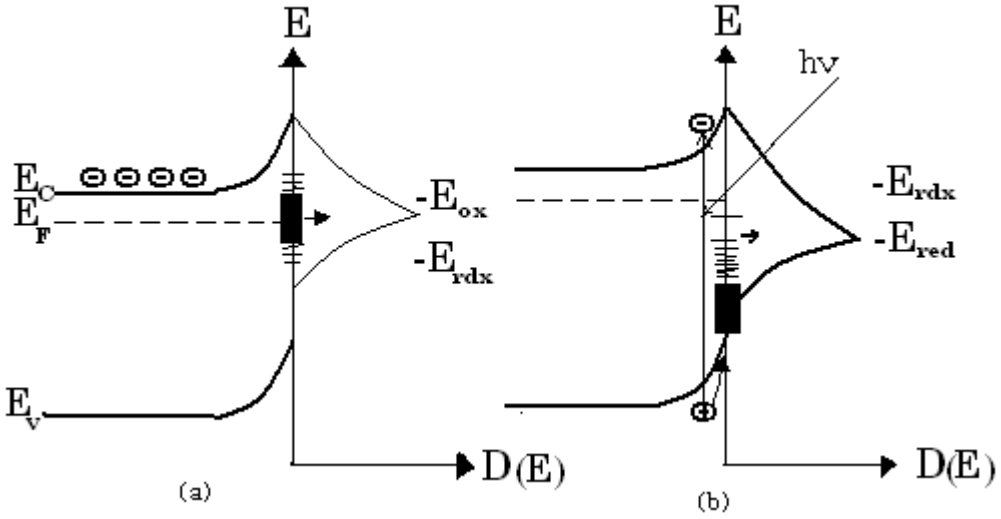

Figure (1.11): Mediation of charge transfer by surface state at n-type SC.
a) Majority carrier injection through the barrier produced by band bending.
b) Photo-generated minority carrier injection via surface state.

iii) Doping Instability

If an electrode is biased in the depletion layer, very strong electric fields are present in it. The field can act on charged donor and acceptor doping species, causing them to migrate slowly in the crystal lattice. After

several hours or days of use, the doping density becomes inhomogeneous near the electrode surface [48].

1.14 Types of Solar Cells:

a) Mono-Crystalline Electrodes:

They are the most developed and prevalent type in use today. These include single crystal and polycrystalline silicon which is either grown or cast from molten silicon and later sliced into desired cell size. These wafers are then assembled onto a flat surface and covered with a protective tempered glass surface. Single crystal silicon cells have the highest average efficiency for converting solar energy into useful electricity. Polycrystalline silicon cells, though a bit less efficient, are less expensive to manufacture [49].

b) Thin Films or Amorphous Electrodes:

They are inherently cheaper to produce than crystalline silicon but are not efficient. They are produced by depositing a thin layer of photovoltaic material onto a substrate like glass or metal. This material can be encapsulated in building materials such as shingles to readily building-integrated photovoltaic systems. Solar roofing materials allow PV to be used in some circumstances where glass covered solar panels would not be

permitted or would be impractical. Solar shingles and roofing material tend to be a bit more expensive than crystalline solar modules per quantity of power produced [50].

1.15 Advantages and Disadvantages of PEC Cells:

There are several ***advantages*** of PEC cells for solar energy conversion over PV devices:

(a) Energy can be stored in PEC devices in the form of conventional fuel.

(b) PEC cells do not contain solid-solid junctions and easy to fabricate.

(c) No problems occur in PEC cells due to thermal expansion as in PV solid- solid junctions.

(d) No antireflection coatings are required in PEC cells [51].

The ***disadvantages*** of PEC cells are:

a) The absorption of light by the electrolyte solutions, b) Reflection losses from the cell, and c) The unstability of the electrode. All these lower the efficiencies in PEC cells [52].

1.16 Types of SC Materials for PEC Cells

The absorber material of SC in solar cell should be with acceptable price. The following requirements should be fulfilled:

1) The band gap of the SC should be suitable for using maximum part of solar spectrum.

2) The efficiency of the cell should be high which depends upon conductivity, diffusion length, band gap, surface state, etc.

The diffusion length is a measure of how far the doping density has propagated in the substrate by diffusion in time *t* [53].

3) The electrode must be stable against corrosion when placed in redox couple [54].

The most SC's used in solar cells: are (Ge and Si), III-V compound (GaP, InP, GaAs), II-compound (CdSe, CdS, CdTe), Transition metal di-chalcogenides ($MoSO_2$ and ZrS_2), Oxide semiconductors (TiO_2, WO_3 and ZnO), Zinc phosphides (Zn_3P_2), and Ternary compounds ($CuInS_2$ and $CdIn_2Se_4$) [55].

1.17 Earlier Studies on CdSe:

A number of techniques are employed in the formation of high quality thin films such as, chemical vapor deposition, molecular beam epitaxial, pulsed laser, evaporation and sputtering. Chemical bath deposition (CBD) and electro-deposition techniques are belonging to these alternative methods that could also produce high quality films of chalcogenied materials. Effect of many parameters on characteristics of CdSe thin films deposited by CBD, were studied by G. Sarfa [56]. The variation of CdSe crystallite size with annealing temperature is shown in Figure (1.8) [57].

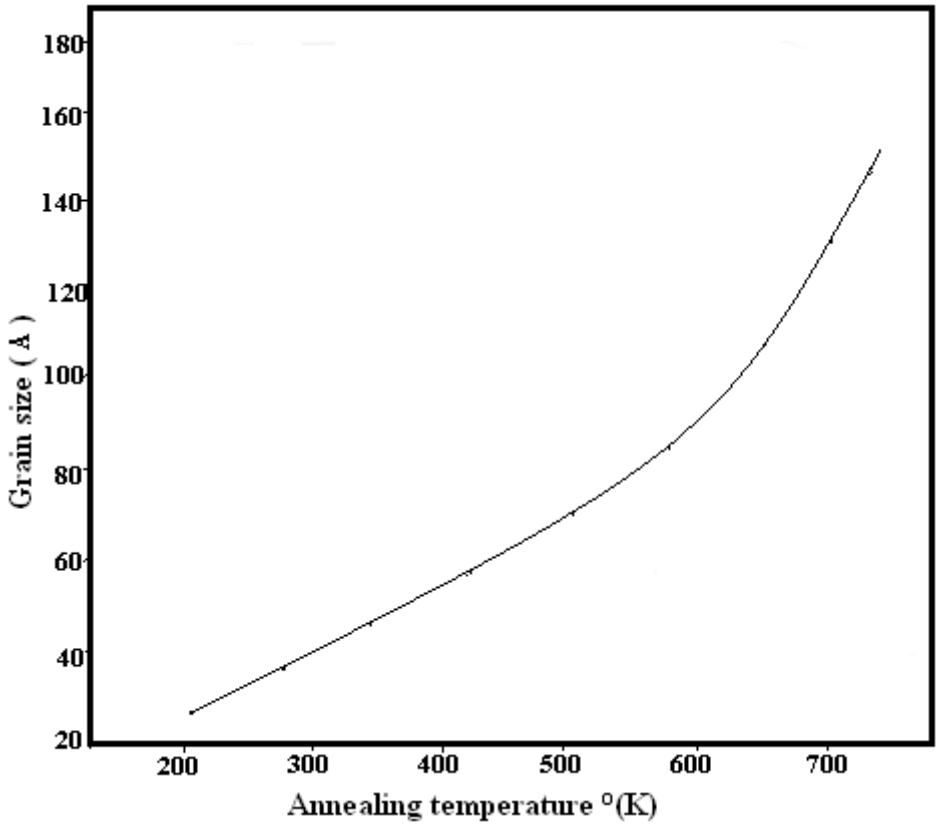

Figure (1.12): Plot of CdSe crystallite size vs. annealing temperature of CdSe thin films deposited by CBD technique [57].

The thickness evolution with time of the deposited layer is shown in Figure (1.9). Annealing of thin films of CdSe has been studied by V. M. Garcia [58]. Controlling the size of nanocrystals of CdSe was achieved by changing the intensity of light illumination of growing film. The nanocrystals radii were found between 1.9-10 nm.

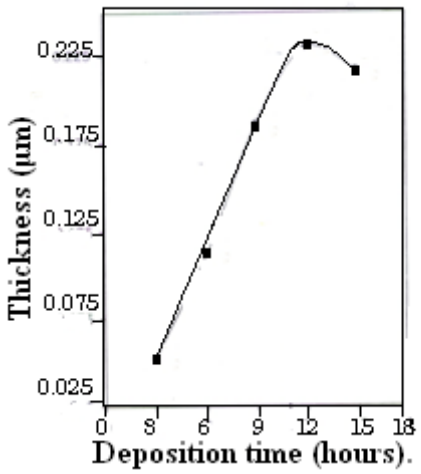

Figure (1.13): Variation of CdSe film thickness with deposition time[59].

The effect of deposition parameters on the optical and electrical properties of nanocrystalline CdSe was reported by Charita Mehta and coworkers [60]. Analysis of optical absorption data to find the band gap has been reported in the literature [61-64]. Other workers studied the improvement of the prepared films by modification of the CBD preparation procedure. The characteristics of the prepared films were investigated by measuring their optical properties, structural morphology and chemical composition

[65]. The effect of parameters such as bath composition, deposition temperature, pH of the solution, speed of the rotation and the specificity of complexing agent on growth process was studied [66]. Scanning electron microscopy (SEM) is a technique to study microstructure of thin film Figure (1.10), (a) and (b) shows the SEM micrographs of as-deposited and annealed at 673 K of CdSe thin films.

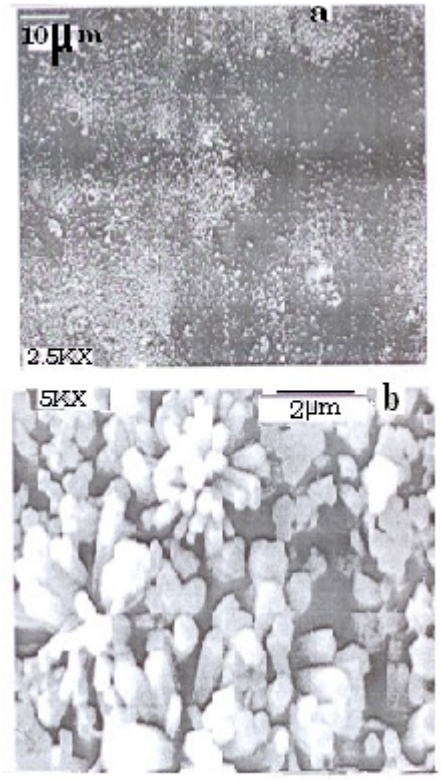

Figure (1.14): SEM of CdSe thin films (a) as-deposited and (b) annealed at 673 K [67].

From SEM studies, it is observed that the as–deposited CdSe films are nanocrystalline, homogeneous without cracks or holes and well covered to the glass substrate.

Despite that, to our knowledge there are many important studies that have not been conducted on CdSe thin films. Examples of such studies are:

1) Deposition of CdSe thin films onto FTO glass by CBD.

2) The PEC study of CdSe films on FTO, prepared by CBD.

3) Effect of cooling rate on CBD made CdSe films, on FTO, on its characteristics.

4) Surface modification of CdSe film electrodes, prepared by CBD onto FTO.

1.18: Major Theme of This Study:

The major themes of this study are:

1) Preparing CdSe thin films deposited onto FTO glass by CBD.

2) Trying to use CdSe films deposited onto FTO/glass substrates as electrodes in light –to-electricity conversions under PEC conductions.

3) Trying to enhance CdSe thin film electrode efficiency and stability by controlling cooling rate of pre-annealed samples.

4) Coating the CdSe thin film electrodes with electroactive metalloporphyrine complex embedded in polysiloxane polymer matrices and investigate the effect on their PEC characteristics.

5) In parallel to PEC characteristics, effect of treatment on other properties such as absorption spectra and photoluminescence emission spectra will also investigated.

Chapter Two

Experimental Work

2.1 Materials

2.1.1 Chemicals and Solvents

Starting materials, such as Se, S, $K_3Fe(CN)_6$, $K_4Fe(CN)_6$, $LiClO_4$, KOH, $CdCl_2.2H_2O$, Na_2SO_3, Na_2S, were purchased from Aldrich, HCl was purchased from Frutarom, and methanol from Riedel-DeHaën.

2.1.2. Preparation and Characterization of MnP:

The tetra(-4-pyridy1)porphyrinatomanganese(III)sulfate (MnP) complex, Figure (2.1), was prepared from H_2TPyP (81.7 mg, 0.132 mmol) was vigorously refluxed with excess manganese (II) sulfate (1.53g, 0.91 mmol) in N, N-dimethylformamide, DMF, (60 ml) for 10h. The solution was concentrated by evaporating DMF under reduced pressure. Air was passed through the reaction mixture to oxidize Mn^{2+} to Mn^{3+}. The reaction mixture was then ion-chromatographed over activated neutral alumina using DMF as eluant. Eluate fractions with the characteristic absorption bands at 462, 569 and 620 nm, [68], were stored in the dark [69].

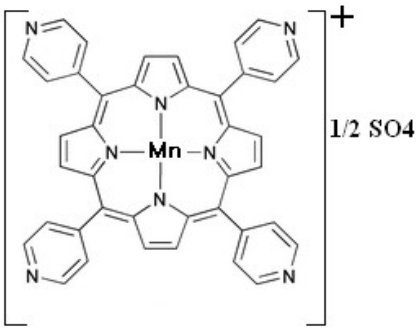

Figure (2.1): MnP polymer [70]

The mixture contained complexes of both the Mn^{II} and the Mn^{III} , as depicted from the electronic absorption spectra in the visible region, Figures (2.2-2.5).

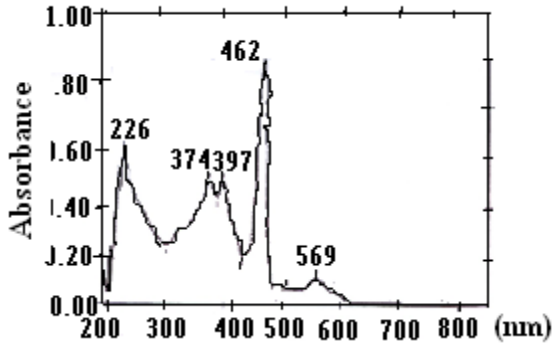

Figure (2.2): The electronic absorption spectra in UV/ visible region for MnP solution in methanol [71].

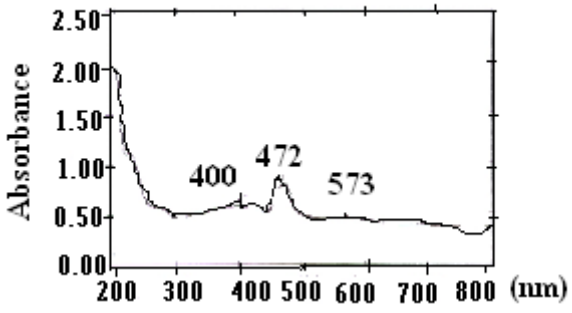

Figure (2.3): The electronic absorption spectra in the UV/visible region for MnP embedded into a polysiloxane polymer solid matrix [72].

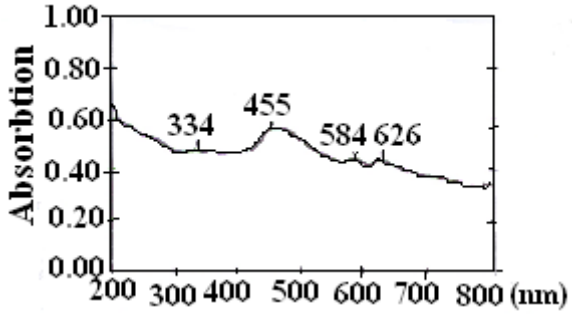

Figure (2.4): The electronic absorption spectra in the UV/visible Region for MnP embedded into a polysiloxane polymer solid matrix after annealing at 150℃ for 30 min. under N_2 atmosphere [73].

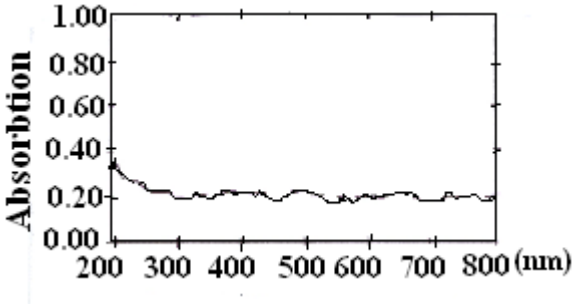

Figure (2.5): The electronic absorption spectra in the UV/visible region for solid polysiloxane membrane [74].

2.1.3 Etching Process

The prepared electrodes of CdSe to be etched were treated by dilute HCl (10%) solution. The electrode was immersed in the dilute solution of HCl for about 5 seconds and then rinsed with distilled water and methanol then dried with nitrogen. The above procedure was for obtaining a shiny film surface.

2.1.4 Preparation of CdSe Thin Films

Chemical bath deposition technique was adopted for the preparation of the cadmium selenide thin films. The deposition of thin films was on glass plates covered by Fluorine-doped Tin Oxide (FTO) thin film. The experimental arrangement is shown in Figure (2.6). It consists of a chemical bath of Na_2SO_3 and Se [75]. Ordinarily, selenium is not soluble in water. In order to create selenium ions in the form of sodium selenosulphite (Na_2SeSO_3), selenium powder was mixed with sodium sulphite solution and heated to 90^0C for about 9 to15 hours. The resulting Na_2SeSO_3 becomes the source of Se^{-2}, while the source of Cd^{+2} is the cadmium chloride ($CdCl_2.2H_2O$). Ammonia was used as a comlexing agent. To prepare 300 ml of Na_2SeSO_3 solution, 60 gm of $Na_2SO_3$was added to 300 ml of distilled water, then 6 gm of Se powder was added to the solution. After stirring for 15 hours at 90^0C, fresh Na_2SeSO_3 solution is filtered. In another beaker, 30 gm of $CdCl_2.2H_2O$ was added to 300 ml of distilled water, then 25% NH_3 solution was added to the solution with constant stirring until milky turbid $Cd(OH)_2$. Further addition of excess ammonia dissolved turbidity and made solution clear. To this mixture, 300ml of freshly prepared Na_2SeSO_3 was added slowly with constant stirring [76].

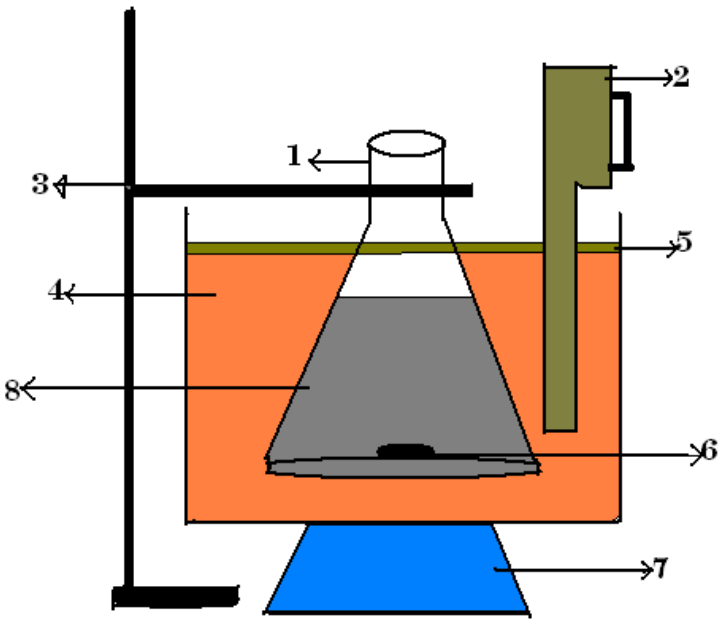

Figure (2.6): Experimental arrangement for preparing Na_2SeSO_3 fresh solution: 1-beaker (500 ml); 2-thermostat, 3-holder, 4-disstiled water, 5-layer of paraffin oil, 6-magnetic stirrer, 7-electrical stirrer, 8-chemical bath of Na_2SO_3.

The solution was stirred for 10 seconds and then transferred into another beaker containing cleaned glass substrates of FTO glass that were hanged vertically in the beaker. The bath solution was made in 3 beakers, one was kept at room temperature 300 ^{0}K, the other was heated to 60^{0}C, and the third was heated to 80^{0}C. The substrates were coated with CdSe thin films with intervals 4 hours and12 hours, then washed with water and preserved in a plastic container. The deposited thin films were uniform well adherent to the substrate and red orange in color. Two depositions were made for all the electrodes that were used in the experiments unless otherwise stated.

2.1.5 Annealing Process

Annealing was conducted using a thermo stated horizontal tube furnace. The prepared CdSe film substrates were inserted in the middle of a long Pyrex cylinder. The heat was raised to the desired temperature (100,150, 200, 250, 300, 350) ^{0}C, under air pressure. The sample was kept at that temperature for 20 min before being allowed to cool. The annealing system was shown in Figure (2.7).

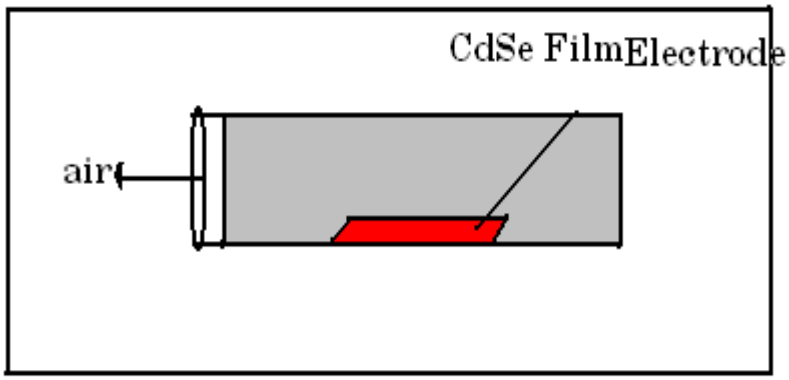

Figure (2.7): The annealing system

2.1.6 Cooling Process

a) Quenching (Fast Cooling)

The furnace was switched off. The heated system (Pyrex cylinder and film substrate) was taken from the furnace left to cool under air from the desired temperature to room temperature within about 3 minutes.

b) Slow Cooling Process:

After 20 min of heating at desired annealing temperature, the oven temperature was lowered by 50 ^{0}C. After the reading temperature reached the setting temperature, the oven temperature was lowered by 50^{0}C, again. This procedure was repeated until room temperature was reached, through step –wise process, with 50^{0}C lowering in each step. Rate of cooling was 100 ^{0}C per hour on the average.

2.2 Equipment

2.2.1 Measuring Devices

The measurements of current –voltage data were performed using a computer controlled Princeton Applied Research (PAR) Model 263A potentiostat. Light intensity was measured with Lutron –LX 102 light meter. The light meter, which measures the luminance in lux units, was calibrated against a Kipp and Zonen CM11 pyranometer. UV absorption spectra were measured on a Shimadzu UV-1601 spectrophotometer. PL emission spectra were measured on a Perkin Elmer LS50B Luminescence spectrometer Figure (2.8). PL spectra of films of CdSe on FTO glass where directly measured using excitation wavelength 250 nm.

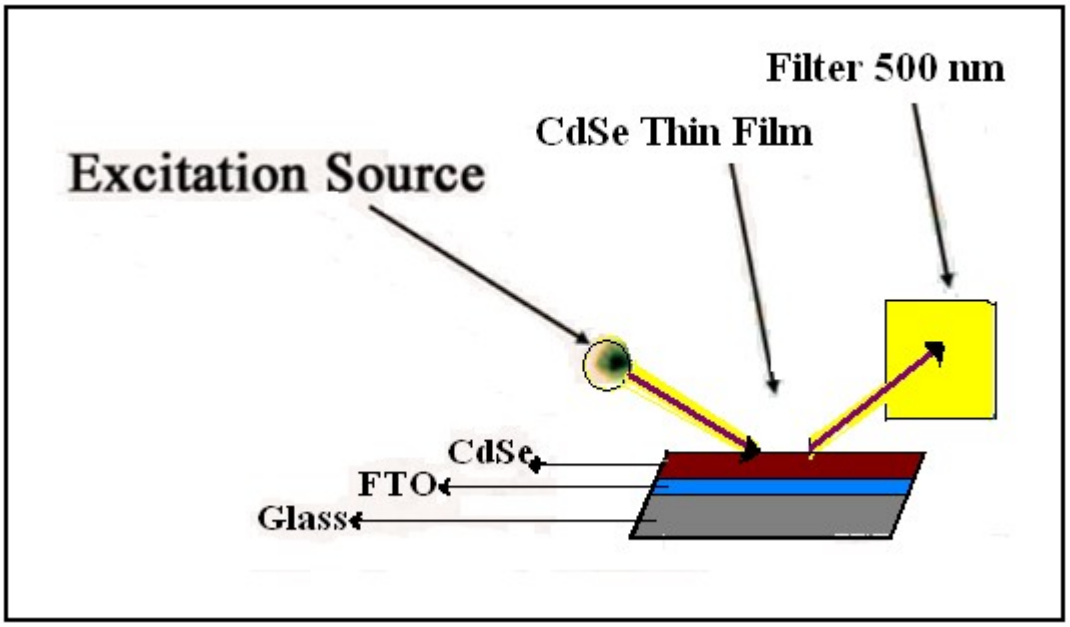

Figure (2.8): Schematic diagram showing measurements of the PL emission spectra using Perkin Elmer, luminescence spectrometer LS50B.

2.2.2 PEC Cell

The prepared CdSe film electrode was incorporated as a working electrode into a three–electrode one-compartment photoelectrochemical cell, with a platinum counter electrode and reference saturated calomel electrode, SCE, Figure (2.9). Two types of electrolyte solutions were used in this work. The first was: 0.1M of $LiClO_4$, 0.05 M of $K_3Fe(CN)_6$ and 0.05 M of $K_4Fe(CN)_6$. The second was: 0.1 M of (Na_2S, S, KOH), all in distilled water. In each case high purity nitrogen (99.999%) was bubbled through the solution for at least 5 minutes before each experiment, and was kept to bubble over the solution during the experiment to minimize contamination with air.

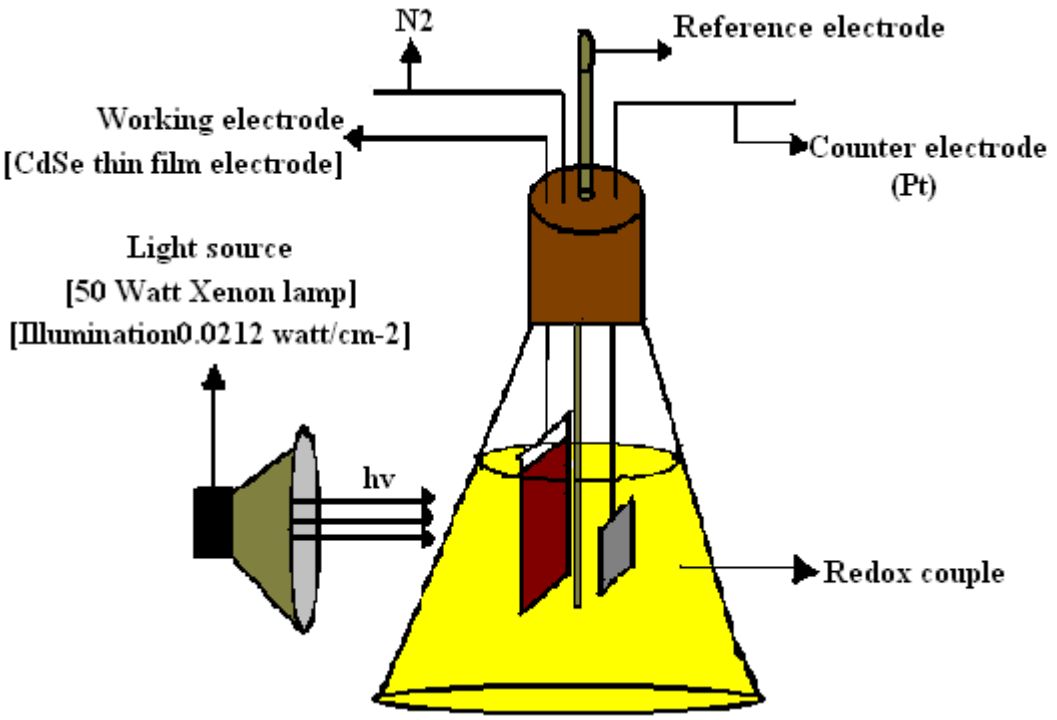

Figure (2.9): Three electrode photoelectrochemical cell (PEC).

2.2.3 Light Source

For illumination 50 watt Xenon lamp was used, with a housing and a concentrating lens. This lamp has an intense converge of wide spectral range between (450-800) nm with a high stability. The lamp was placed at a certain distance from the working electrode. The illumination power on the electrode was about 0.0212 W. cm^{-2}.

2.3 PEC Measurements

2.3.1 Current Density –Potential Plots

Current density (J-V) plots were measured using the PEC cell shown in Figure (2.8), at room temperature. Nitrogen atmosphere was kept above the

solution. The photocurrent measurements were done using a 50 watt Xenon lamp; but the dark current ones were done under complete dark using thick blanket cover. The measurements of current –voltage data were performed using a computer controlled Princeton Applied Research (PAR) Model 263A Potentiostat/Galvanostat. The measured current (I) was converted into current density (J), by dividing the current I by the area of the illuminated electrode.

2.3.2 Stability Testing

Using the same PEC, short circuit current density (I_{sc}) values were measured over a range of time periods. Short circuit current density(J_{sc}) were calculated by dividing values of I_{sc} by electrode area (cm^2). The light was maintained during the measurements on the electrode, with steady illumination (0.0212)$W.cm^{-2}$, and under 0.00 V bias, at room temperature. Effect of electrode annealing and cooling rate were studied.

2.4 UV/Visible Absorption Spectra Measurements

UV absorption spectra were measured for substrates annealed at different temperatures. Some of the electrodes were quenched, others were slowly cooled, and one was not annealed. A Shimadzu UV-1601 spectrophotometer was used for absorbance measurements. Gas

Chromatography/Mass Spectrometry analysis was conducted on a Shimadzu GCMS-QP 5000.

2.5 Photoluminescence (PL) Emission Spectra

Photoluminescence emission spectra were measured for different substrates:

a) For substrates annealed at different temperatures (100, 200, 350) ^{0}C, slowly cooled and one not annealed, all prepared at room temperature.

b) For substrates annealed at (100, 200, 350)^{0}C, quenched and one not annealed, all prepared at room temperature.

All the measurements were made with excitation 250nm. A cut off filter (shorter than 500 nm removed) was used between the sample and the detector.

2.6 Coating The Electrodes With a Polymer

In order to enhance CdSe film contact with FTO, the glass/FTO electrodes were gently polished with fine glass paper. This was to allow better contact between CdSe films with FTO.

Covering the electrodes with a polymer was conducted as follows: A dilute solution, of commercial RTV made polysiloxane paste in acetic acid, was prepared by dissolving 0.01 mg of the paste in 20.0 ml of

dichloromethane. Similarly, an MnP solution was prepared by dissolving (0.01 mg, 1.38×10^{-5} mol) in 1.0 ml methanol. The MnP/polysiloxane stock solution was prepared by adding the MnP solution to the polysiloxane solution in a 1:4 (V/V) ratio, respectively. Then 0.1 ml of the MnP/polysiloxane stock solution, containing 4.0×10^{-5} g polysiloxane and 2.0×10^{-4} g MnP, were coated onto the preached CdSe polished surface. The substrate was immersed in the solution for 4 seconds. The organic solvent mixture, dichloromethane/methanol, was then allowed to evaporate off, leaving a transparent thin layer of MnP/polymer matrix on the surface of electrode. With thicker films than 4 μm, the polymer matrix worked as insulator and allowed no current to be measured. All SC electrodes were coated using thickness about 4μm. In control experiments, CdSe surfaces were modified with a thin polysiloxane film and MnP. The modified electrode was further annealed, after fabrication, at 100^0C for 30 min under nitrogen. The system was then left to cool at room temperature under N_2 [77].

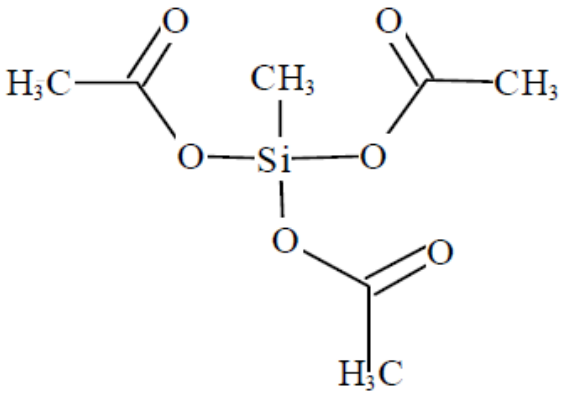

Methyltriacetoxysilane

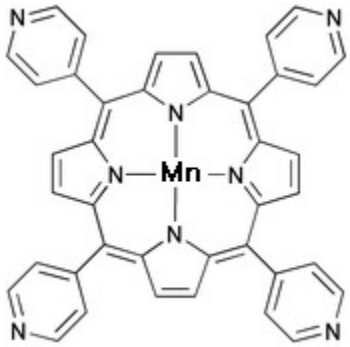

Tetra-4 pyridylporphyrinatomanganese(III) complex.

Figure (2.10): Compounds of the polymer used for coating the CdSe thin films.

2.7 Measuring the Thickness of CdSe Layer

The thickness of the layer was measured by two ways:

1) By optical microscopic measurement which gave approximately less than 20μm thickness.

2) By a micrometer which was (~10 μm).

Chapter Three

Results

General Remarks

Chemical bath deposition technique was used in this work to prepare thin films of CdSe onto glass substrates. The prepared films were treated by annealing at different temperatures, (100,150, 200, 250, 300, 350) ^{0}C under air. Two different methods were used to cool the annealed films to room (~25 ^{0}C) temperature; quenching or slow cooling. Effects of annealing and cooling rate on UV/Visible absorption spectra of the prepared thin films were measured. Treated and untreated films were studied as electrodes in PEC system. The main objective was to see optimal conditions that yield highest electrode efficiency and stability under irradiation. Two redox couple systems were tested in the PEC measurements. In order to enhance efficiency and stability of the CdSe electrodes, they were coated with MnP/polysiloxane polymer matrices. The treated wafers were then used as PEC electrodes for light to-electricity conversion. The treatment affected dark J–V plots, photo J–V plots, SC efficiency and stability.

3.1 Enhancement Studies of Uncoated CdSe Film Electrodes

As reported by [78], thick matrices of MnP/polysiloxane more than 4 μm showed bad J-V plots for current readings. Therefore, thin matrices, about 4 μm thick were made to lower the resistance. Figures (3.17-30) show that

annealing and then coating the surface of CdSe by MnP/polysiloxane matrix enhanced the J-V plots for both dark current and photo current. These two processes also enhanced the stability and efficiency of CdSe thin wafers.

3.1.1 UV/Visible Absorption Spectra:

Figure (3.1) shows the UV/Visible spectra for the untreated CdSe film. Figure (3.2) shows absorption spectra measured for pre-annealed CdSe thin films at 100^0C, quenched and slowly cooled samples. The Figures indicate that pre-annealing CdSe films gives better absorption spectra with well defined sharp absorption bands. This indicates that pre-annealing, at 100^oC, enhances physical properties of CdSe mictocrystals, despite cooling rate. The slope at right side in Figure (3.1) is not good.

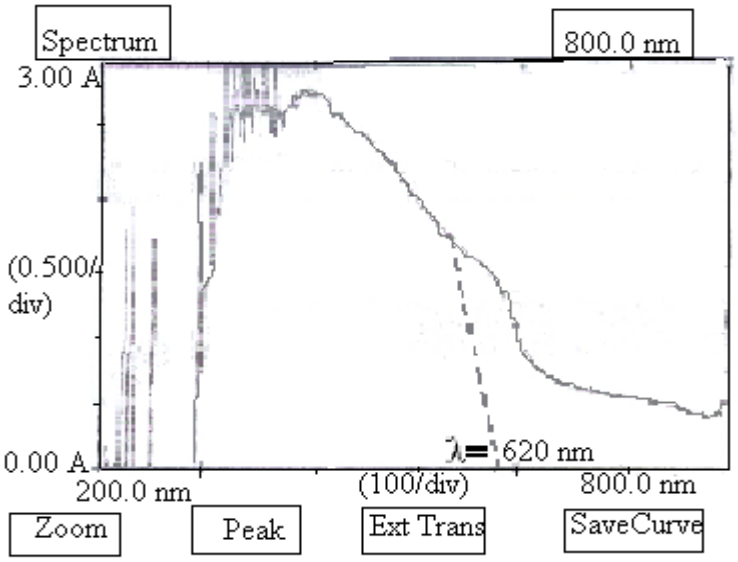

Figure (3.1): UV/Visible absorption spectra, for nonannealed CdSe thin film.

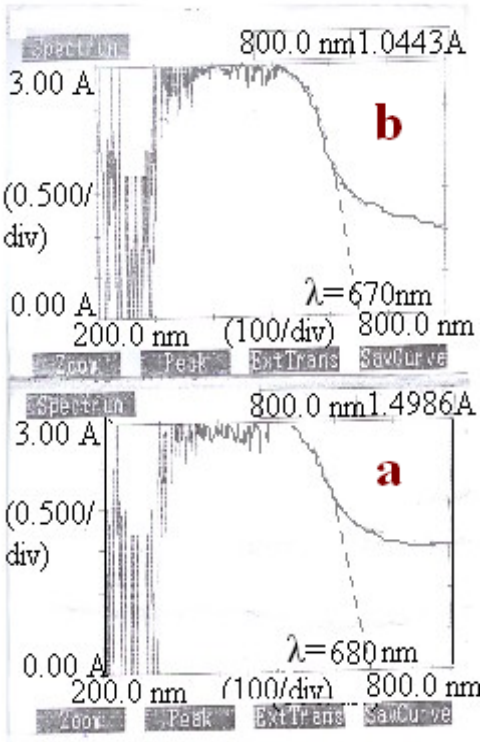

Figure (3.2): UV/Visible absorption spectra for CdSe films annealed at 100 ^{0}C, (a) slowly cooled, and (b) quenched.

Figure (3.3) shows the absorption spectra for CdSe films pre-annealed at 200^{0}C, quenched and slowly cooled. Figures (3.3-a) and (3.3b) indicate that pre-anneled samples at 200^{o}C (both quenched and slowly cooled) show better spectra than unannealed counterpart Figure (3.1). Quenched samples have well defined slope better than slowly cooled ones. Moreover, pre-annealing at 200^{o}C gave better absorption spectra than pre-annealing at100^{o}C, Figure (3.2).

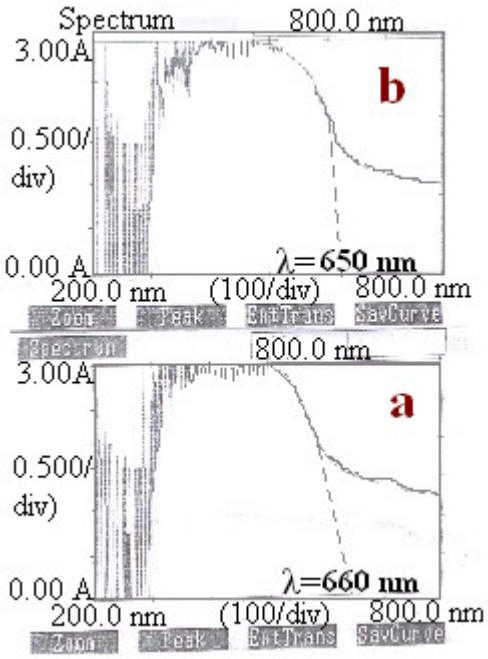

Figure (3.3): UV Absorption Spectra, CdSe annealed at 200 ^{0}C,
(a) slowly cooled, and (b) quenched.

Figure (3.4) indicates that UV-absorption spectra for CdSe electrodes, pre-annealed at 350^{0}C did not show singificant enhancement compared to un-annealed counterpart. The Figures show that annealing at 200^{o}C gives samples with best absorption spectra.

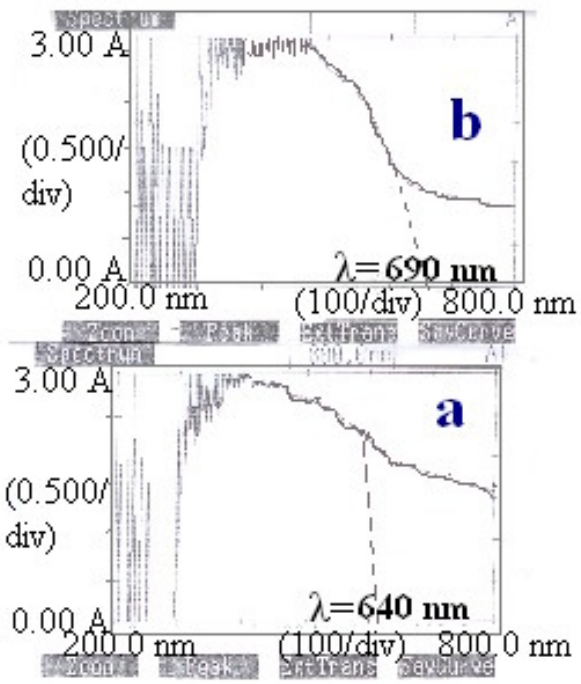

Figure (3.4): UV-Absorption Spectra for CdSe electrode, annealed at 350 ^{0}C, (a) slowly cooled, and (b) quenched.

The band gaps for CdSe films were calculated from UV-spectra as shown in Table (3.1). A line which is extrapolated to the slope at right side of each spectrum, has an intersection with the x-axis. This intersection gives λ. Then: $E_g = 1240/\lambda$ This is done for each value of E_g. Annealing showed lowering in band gap value, from 2.0 to 1.7 eV measured for CdSe films deposited onto FTO glass surfaces here. Literature showed lowering from 2.3 to 1.8 eV by annealing CdSe deposited onto glass substrates [79].

Table (3.1): Band gap values, for CdSe thin films, measured from UV/Visible spectra.

Prepared CdSe thin film.	**Band gap " Eg" (eV).**	**Band gap" Eg" (eV) deposited onto glass [70].**
Non-annealed	**2.0**	**2.3**
100 C (quenched)	**1.85**	**2.0**
100 C (slowly cooled)	**1.83**	**-**
200 C (quenched)	**1.91**	**1.8**
200 C (slowly cooled)	**1.88**	**-**
350 C (quenched)	**1.80**	**1.7**
350 ℃ (slowly cooled)	**1.94**	**-**

Figures (3.2) – (3.4) show that cooling rate affects UV/Visible absorption spectra for CdSe films. In each annealing temperature, the quenched samples showed better spectra with more defined absorption.

3.1.2 Photoluminescence Emission Spectra:

Figure (3.5) shows the PL emission spectra for untreated CdSe film as in Figure (3.5-d) spectrum. PL spectra for annealed (quenched) CdSe films at

temperatures 100℃, 200℃ and 350℃, are shown in curves (c, a and b) in Figure (3.5) respectively. The spectra in Figure (3.5) indicate that pre-annealing CdSe films gives higher emission intensity than the non annealed films. The sample annealed at 200℃ has the best spectrum with highest emission intensity. This indicates that pre-annealing enhances physical properties of CdSe mictocrystals, despite cooling rate. Figures (3.5) and (3.6) show that cooling rate affects PL emission spectra for CdSe films. For the sample annealed at 200℃, the slow cooling is better than the quenched one. For other annealing temperatures, the quenched samples showed better spectra with higher defined emission intensity.

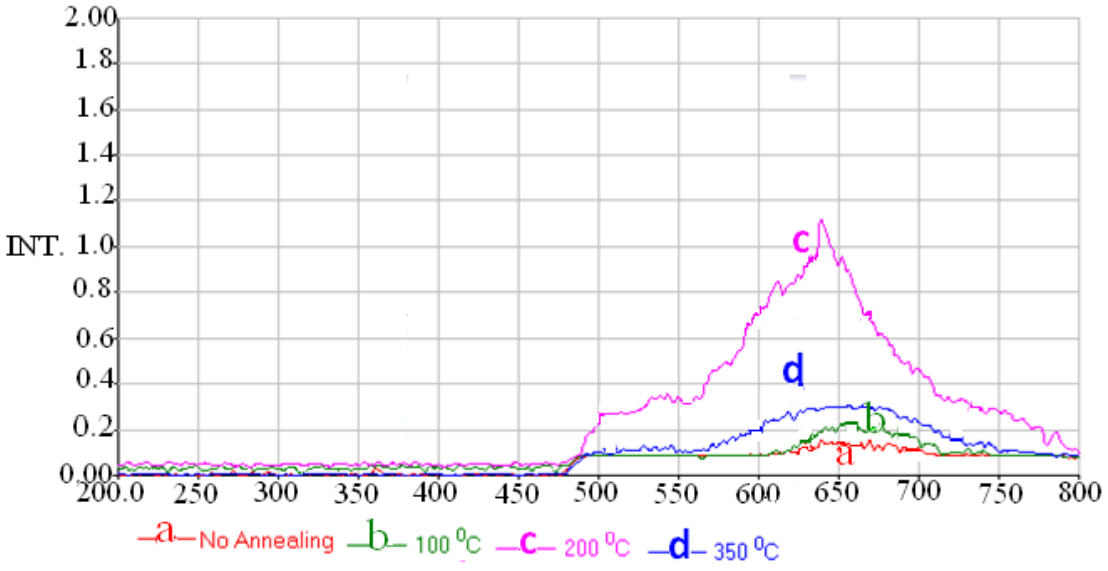

Figure (3.5): quenched thin films, prepared at room temperature.

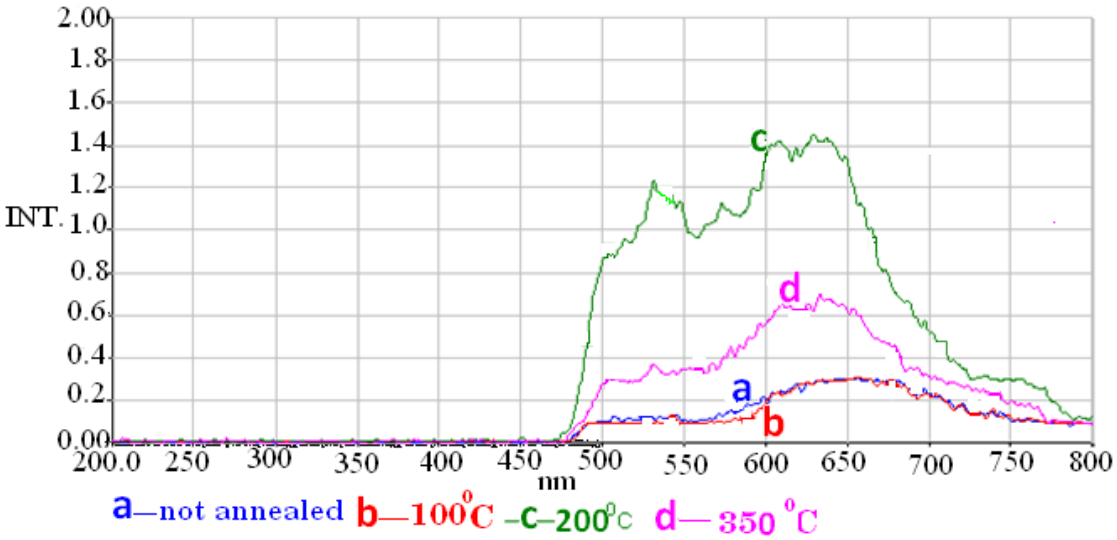

Figure (3.6): Slowly cooled CdSe thin films prepared at room temperature. Filter 500 nm, excitation 250 nm**.**

PL spectra were used to calculate values of E_g for different systems. Where $E_g = 1240/\lambda$, where λ was found from intersection with x-axis by the line from the top of each spectrum. Table (3.2) summarizes these data. The Table shows that annealing at different temperatures did not show significant effect on values of E_g compared to untreated films.

3.1.3 Current Density vs. Potential Plots

The ideal dark J-V plots are plots with sharp appearance of dark current only at onset potential (V_{onset}). Ideal photo J-V plots are curves with 100% fill factor. Figures (3.7) and (3.8) explain these definitions. An ideal photo J-V plot Figure (3.7), is defined as: *a smooth plot in which the filling factor approaches 100%.* An ideal dark J-V plot, Figure (3.8), is defined as: *a smooth plot in which the current density remains zero for a given potential,*

and suddenly it drops negative at the onset potential (V_{onset}).

Table (3.2): Band gap values, for CdSe thin films, calculated from PL emission spectra.

Prepared CdSe thin film	Band gap " Eg" (eV)
Non-annealed	1.90
100 ℃ (quenched)	1.89
100 ℃ (slowly cooled)	1.88
200 ℃ (quenched)	1.94
200 ℃ (slowly cooled)	1.97
350 ℃ (quenched)	1.88
350 ℃ (slowly cooled)	1.97

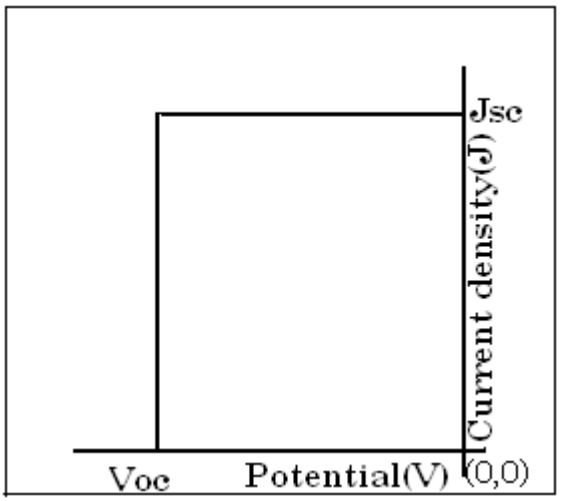

Figure (3.7): Ideal photo J-V plot for SC.

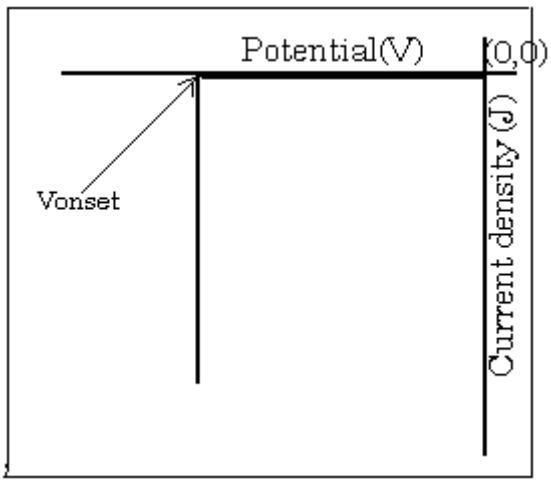

Figure (3.8): Ideal dark J-V plot for SC.

3.1.4 The Effect of Redox Couple

a) Dark J-V Plots for CdSe Electrode

The dark J-V plots for CdSe electrodes were obtained in a redox couple which consists of [$LiClO_4$, $K_3Fe(CN)_6$, $K_4Fe(CN)_6$]. Measurements were performed using unheated electrodes, annealed electrodes at different temperatures, quenched electrodes and slowly cooled ones. Film deposition was conducted at room temperature. The CdSe films were broken down in the solution of the redox couple. All electrodes showed poor dark J-V plots. Figures (3.9)-(3.10) are presented only as examples to show such poor plots.

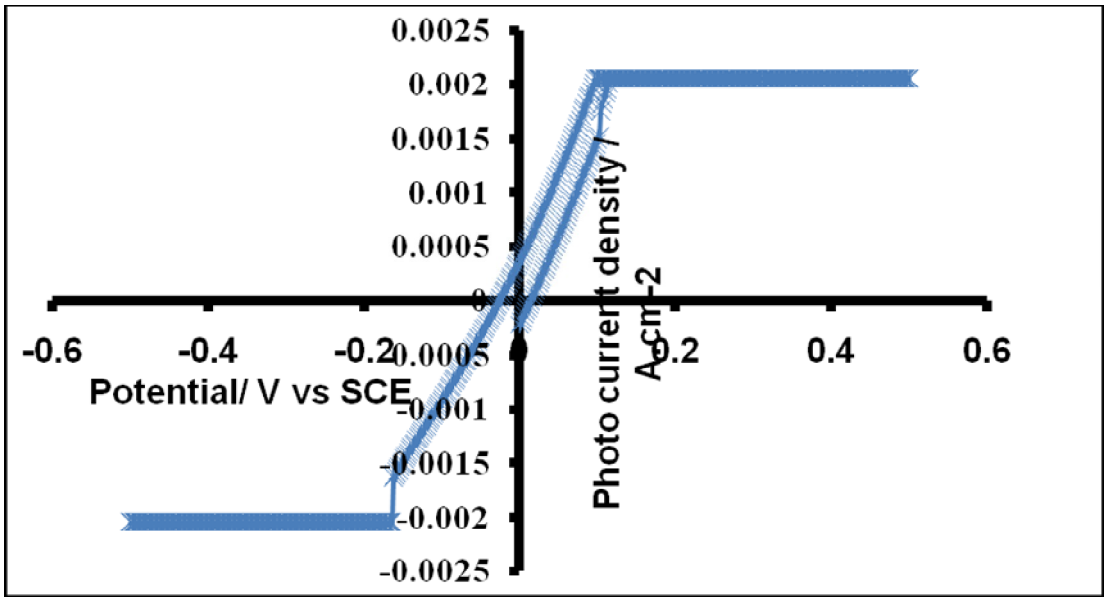

Figure (3.9): Dark J-V plot for CdSe electrode, annealed at 100 ℃ and quenched, in redox solution of 0.1M $LiClO_4$, 0.05M of $K_3Fe(CN)_6$, $K_4Fe(CN)_6$.

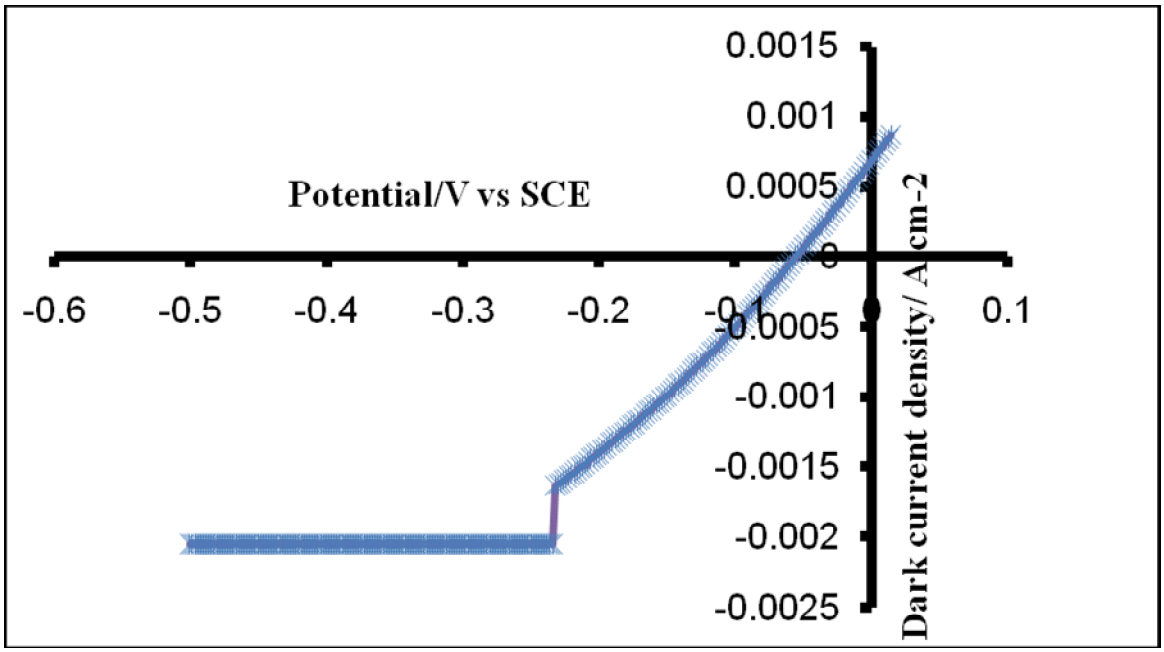

Figure (3.10): Dark current J-V plot for not-annealed CdSe electrode in redox solution of 0.1 M $LiClO_4$, 0.05 M of $K_3Fe(CN)_6$, $K_4Fe(CN)_6$.

b) Photo J-V Plots for CdSe Electrode

Many measurements were performed for nonannealed and annealed CdSe thin films at different temperatures and cooled either by quenching or slow cooling. All measurements for photo J-V plots of CdSe thin films gave so poor results and resembled conductor behavior. No semiconductor behavior was observed. Experiment were conducted in the redox couple system described earlier. Wafers were spoiled, and pieces of them peeled off in the redox couple solution. Figures (3.11)-(3. 12) show examples of some of poor J-V plots.

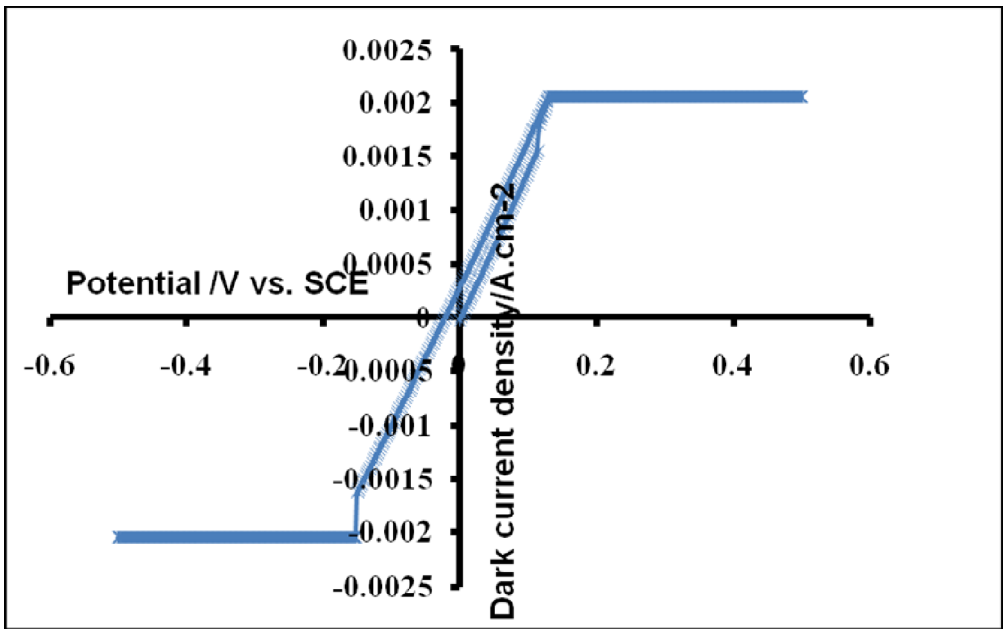

Figure (3.11): Photo J-V plot for not annealed CdSe electrode in redox couple solution 0.1 M $LiClO_4$, 0.05 M $K_3Fe(CN)_6$ and $K_4Fe(CN)_6$.

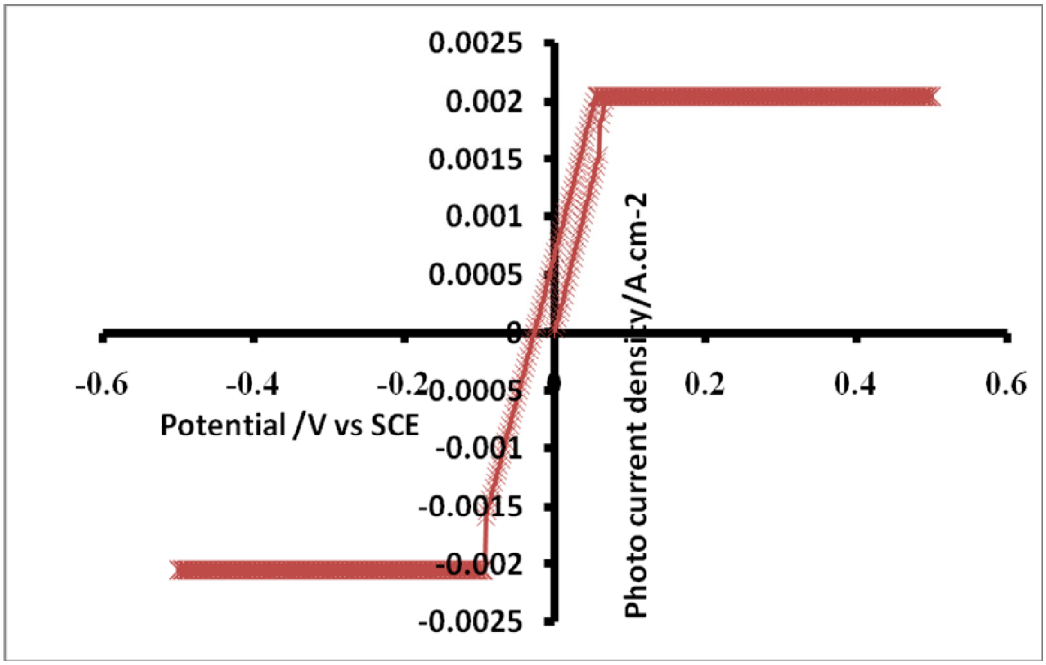

Figure (3.12): Photo J-V plot for CdSe electrode, annealed at 400^0 C, in redox couple solution 0.1 M $LiClO_4$, 0.05 M of $K_3Fe(CN)_6$ and $K_4Fe(CN)_6$.

When another redox couple was used, the results for nonannealed, annealed, (quenched or slowly cooled) CdSe thin films were all poor. The redox couple used was 0.1M of each: S, Na_2S, KOH. Examples of poor

results obtained are shown in Figures (3.13) and (3.14).

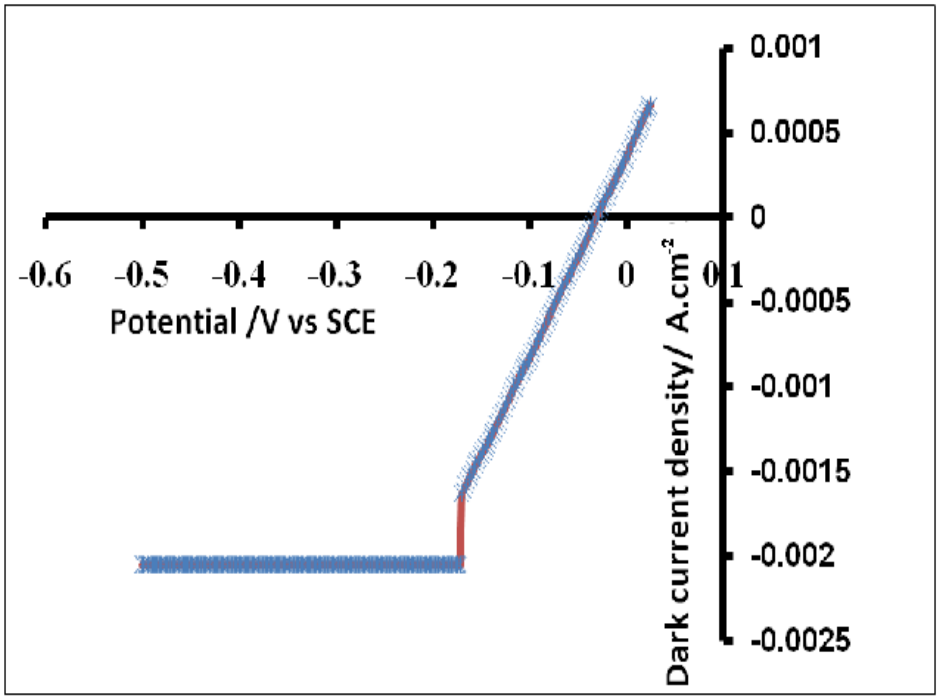

Figure (3.13): Dark J-V plot for CdSe electrode annealed at 350^0C, quenched in 0.1 M (S, Na_2S, KOH).

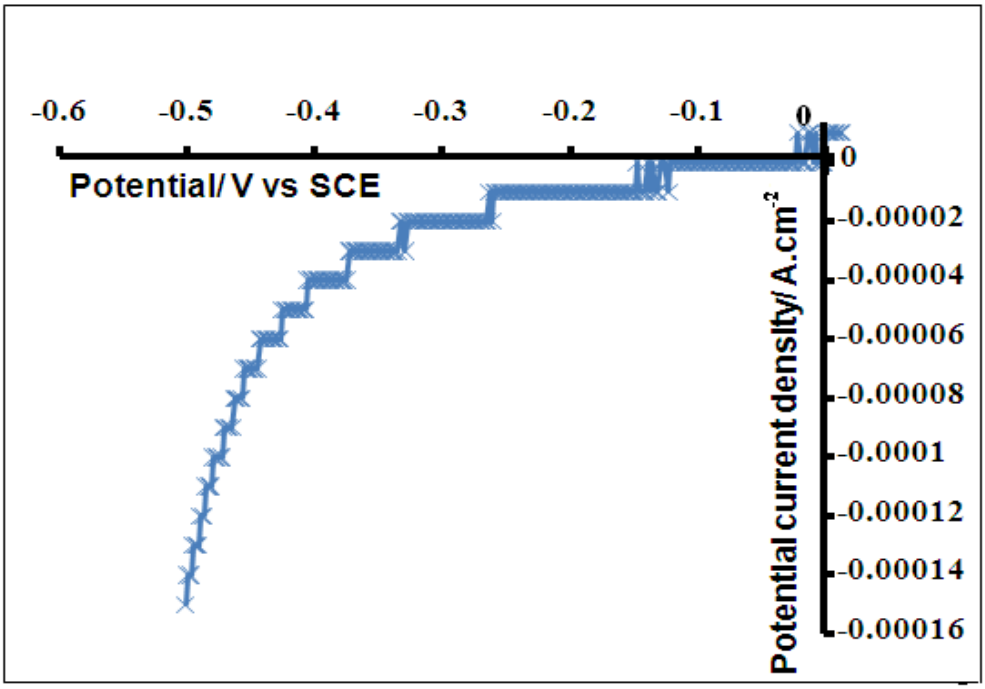

Figure (3.14): Photo J-V plot: not annealed, two depositions, in redox couple 0.1 M of (KOH, S, Na_2S).

Figure (3.15) shows pictures of a number of CdSe /FTO/glass electrodes taken after use in PEC experiments. CdSe peeling off is obvious as complete removal of CdSe films was observed.

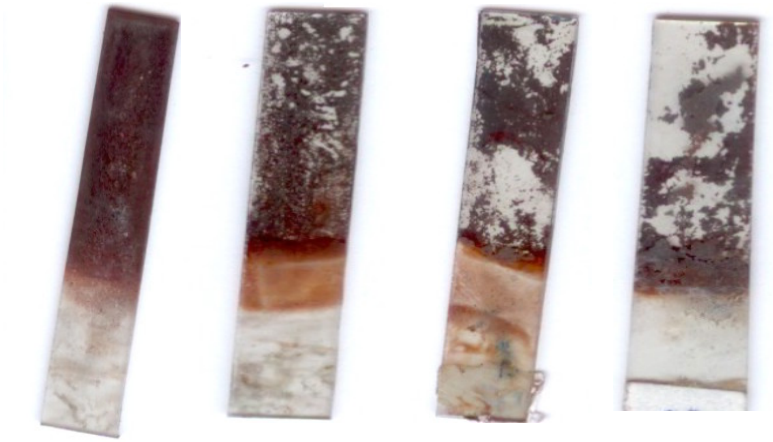

(a) (b) (c) (d)

.**Figure (3.15):** Spoiled electrodes due to the broken down of the CdSe wafer in both redox couples used. a) Not annealed. b) Quenched from 150^0C c) Slowly cooled from 200^0C d) Quenched from 400^0C.

In order to improve contact between CdSe films and FTO, the FTO surface was roughed by fine sand paper, prior to CdSe film deposition. The resulting CdSe/FTO/glass electrode showed some enhancement, and semiconductor behavior was observed, Figure (3.16). However, no significant enhancement was observed, and further modification is needed to be made.

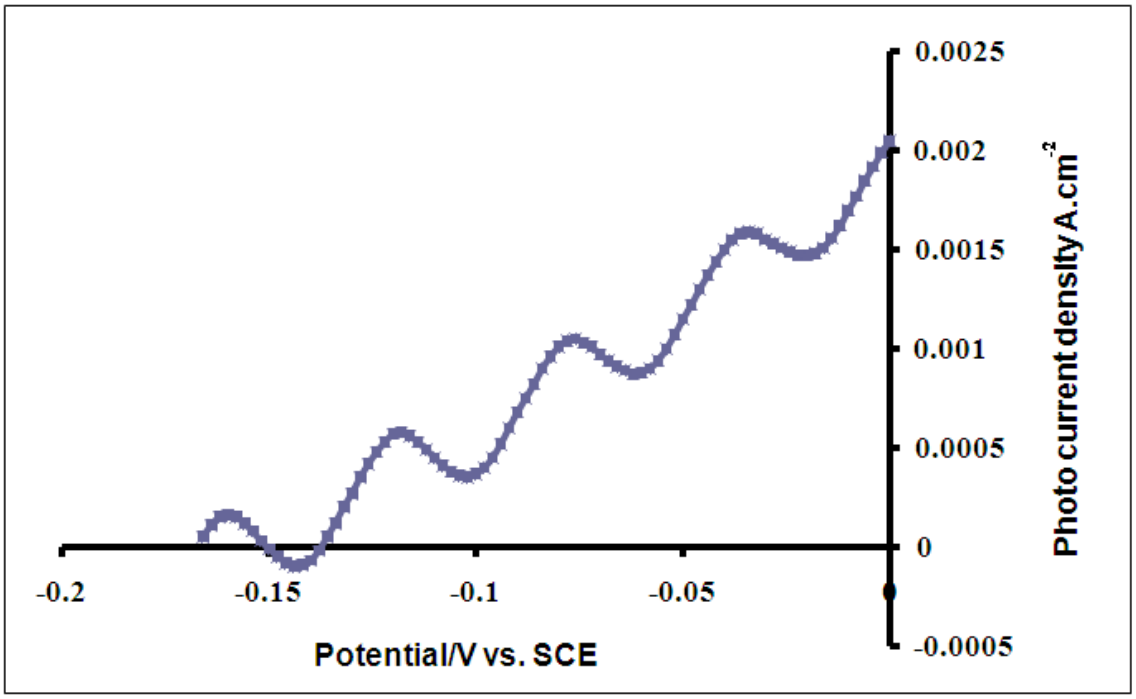

Figure (3.16): Photo J-V plots for CdSe film electrode, annealed to 350^0C, quenched in redox couple 0.1 M (KOH, S, Na_2S). The FTO/glass was treated with sand paper prior to CdSe deposition.

3. 2 Effect of Coating CdSe Thin Films with Mn/Polysiloxane:

Both electrode efficiency and stability of n-GeAs were significantly enhanced by coating the electrodes with porphyrinatomanganese (III and II) couple, MnP, embedded inside polysiloxane matrices [80-82]. To improve adherence of CdSe film, FTO was roughed by fine paper before CdSe deposition, and small enhancement in J-V plots were obtained.

To obtain more enhancement, the electrodes were coated with porphyrinatomanganese (III and II) couple, MnP, embedded inside polysiloxane polymer matrices. The treatment affected dark J–V plots, photo J–V plots, SC efficiency and stability, under PEC conditions.

a) Dark J-V Plots with Polymer

Coating with porphyrinatomanganese, MnP, embedded inside polysiloxane matrices enhances dark current J-V plots for nonannealed electrodes. MnP/polysiloxane-modified electrodes showed better dark J–V plots than uncoated electrodes. The modified electrodes did not peel out in the solution of the redox couple. Figure (3.17) shows that the dark current J-V plots for MnP/polysiloxane modified electrodes show typical diode behaviors in the dark. Pre-annealing of the MnP/polysiloxane modified electrodes at 100℃, 200℃, 250℃, 300℃, 350℃ enhance J-V plots in the dark. These are shown in Figures (3.18-23). Note that CdSe film pre-annealing was conducted before coating with MnP/polysiloxane matrix. After coating with MnP/polysiloxane matrix, each electrode was annealed for 30 minutes, then dried under N_2 atmosphere.

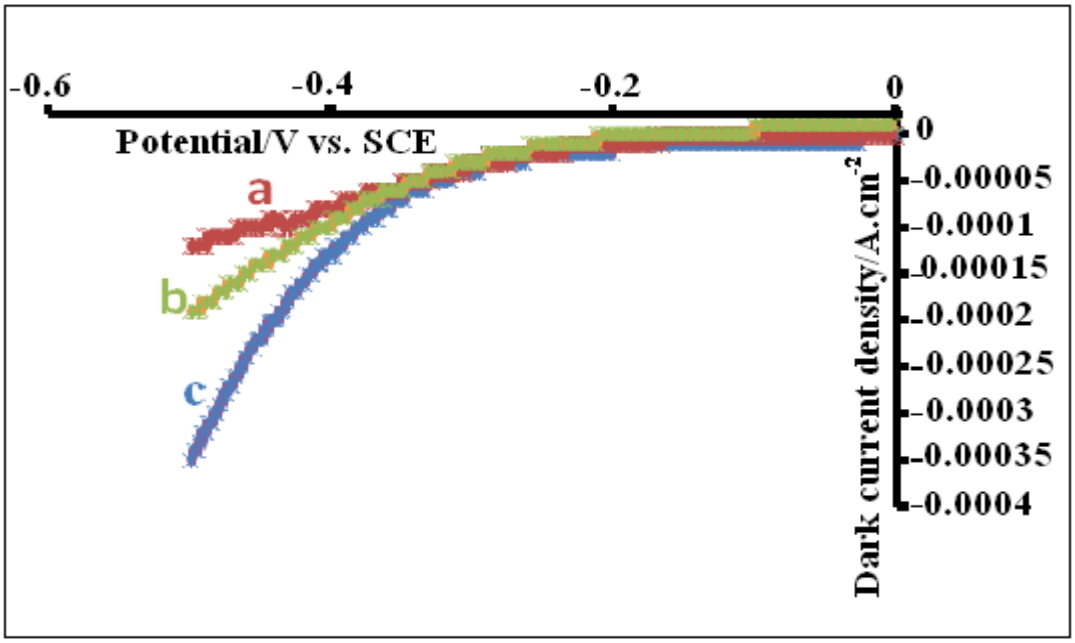

Figure (3.17): Dark J-V plots for MnP/polysiloxane coated CdSe electrodes, (a) unannealed, the others are annealed at 100^0C,
b) slow cooling, c) quenched.

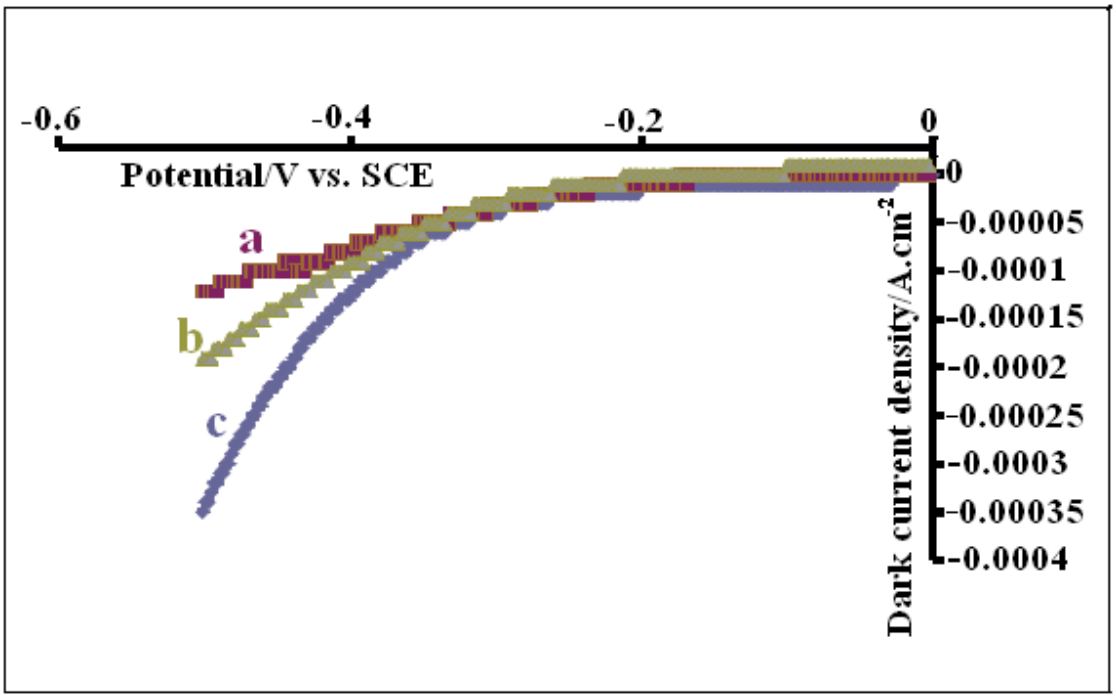

Figure (3.18): Dark J-V plots for MnP/polysiloxane coated CdSe electrodes, (a) unannealed, the others are annealed at 150 ℃,
(b) slowly cooled, (c) quenched.

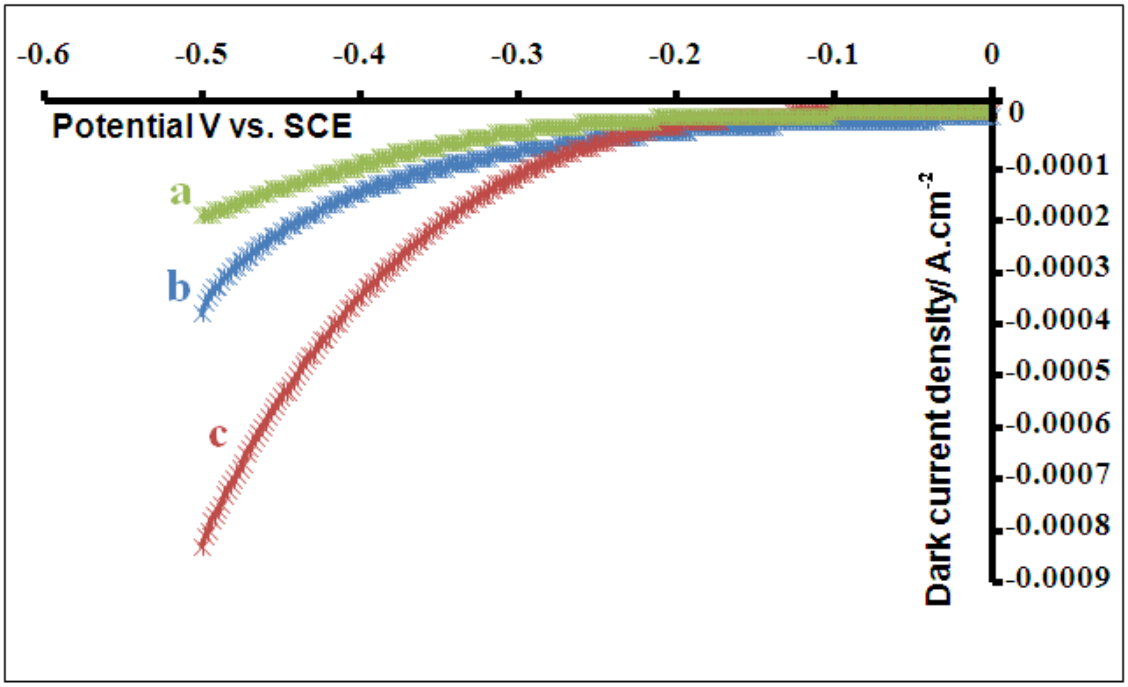

Figure (3.19): Dark current J-V plots for MnP/polysiloxane coated CdSe electrodes (a) unannealed, the others are annealed at 200^0 C, (b) slowly cooled, (c) quenched.

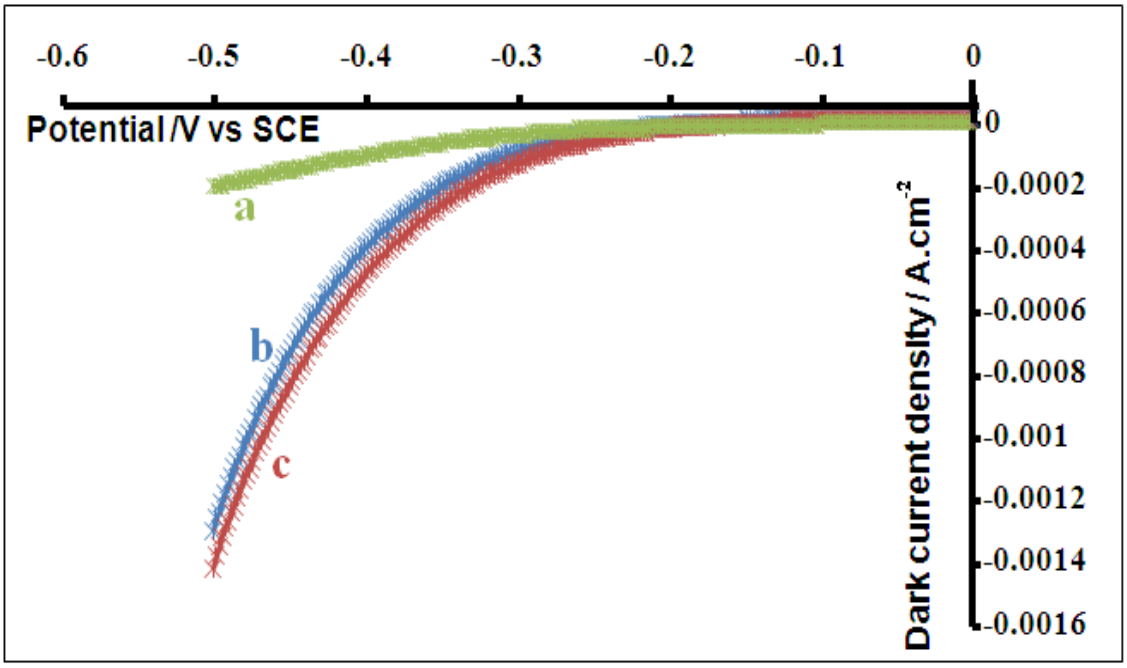

Figure (3.20): Dark J-V plots for MnP/polysiloxane coated CdSe electrodes (a) unannealed, the others are annealed at 250^0C, (b) slowly cooled, (c) quenched.

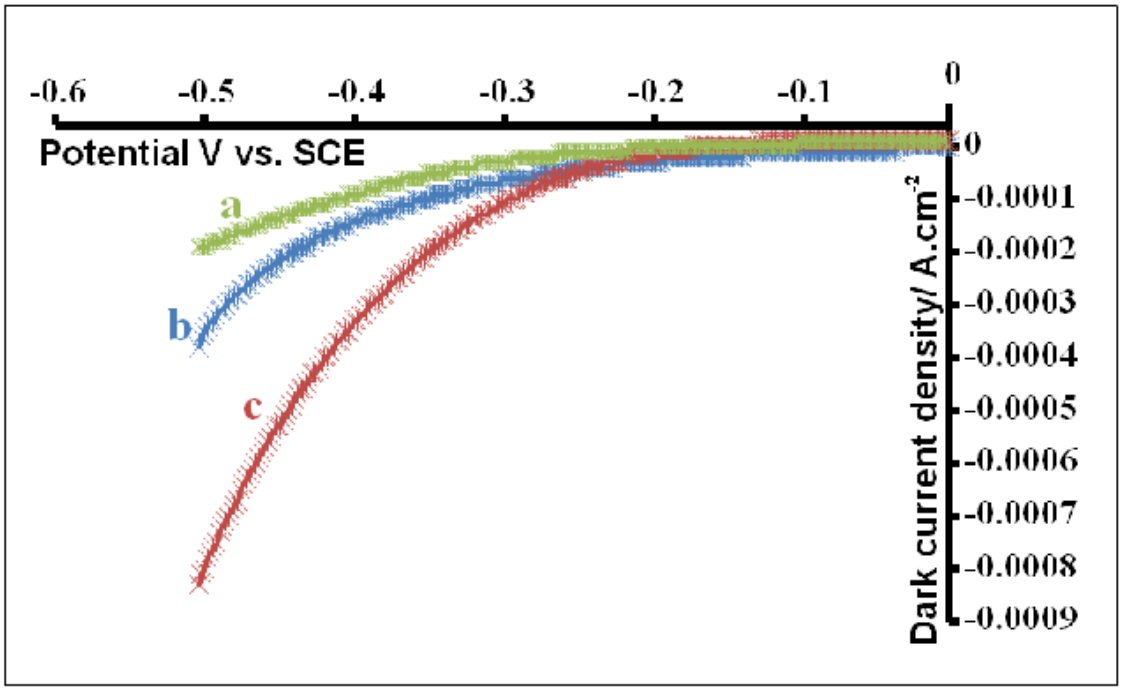

Figure (3.21): Dark J-V plots for MnP/polysiloxane coated CdSe electrodes, (a) unannealed, the others are annealed at 300^0C, (b) slowly cooled, (c) quenched.

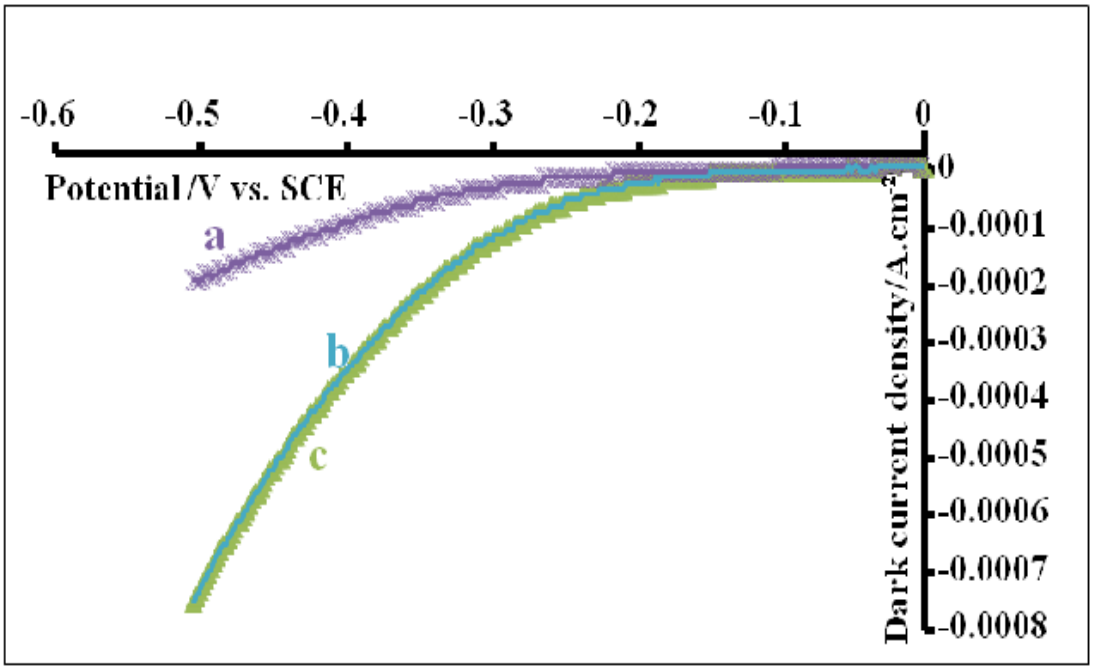

Figure (3.22): Dark J-V plots for MnP/polysiloxane coated CdSe electrodes (a) unannealed, the others are annealed at 350^0C, b) slow cooling, (c) quenched.

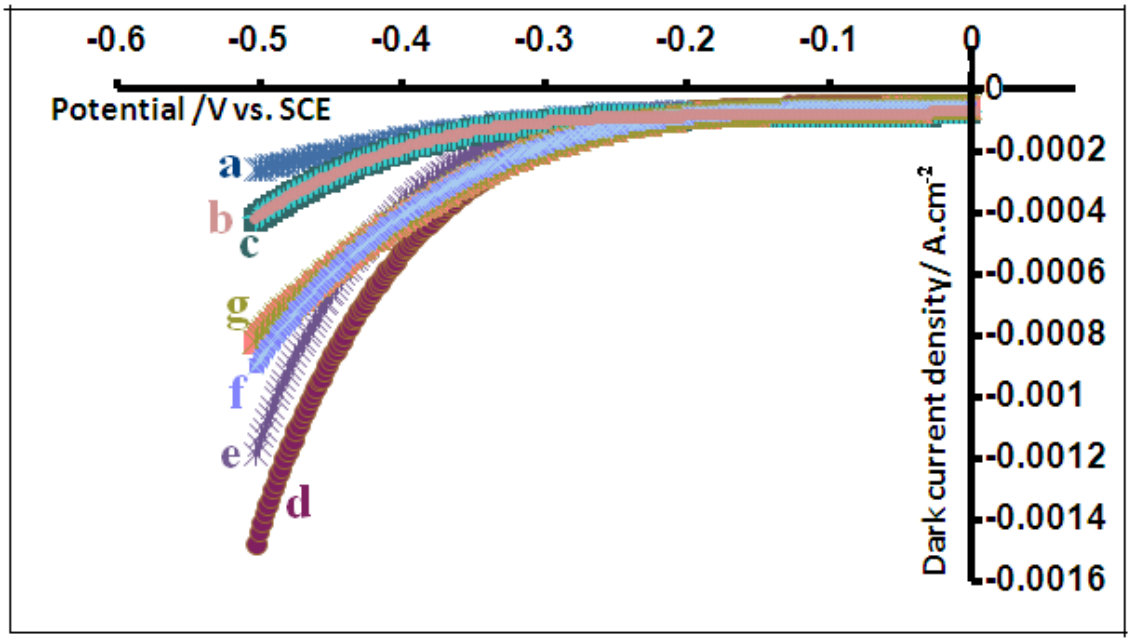

Figure (3.23): Dark J-V plots for MnP/polysiloxane coated CdSe electrodes: (a) un annealed, others are quenched from: b) 100^0C, c) 150^0C, d) 200^0C, e) 250^0C,f) 300^0C, g) $350\ ^0$C.

Figures (3.17) through (3.23) summarize results of dark J-V plots MnP/polysiloxane coated CdSe electrodes.Figures (3.17)- (3.23) indicate that quenched CdSe electrodes, from different temperatures showed better or similar dark-current J-V plots than slowly cooled electrodes. Figure (3.17) shows that slowly cooled and unannealed electrode has aproxematly the same dark J-V plot. Quenched electrpde from 100℃ is better than the slowly cooled and unannealed ones. Figure (3.18) shows that quenched electrode from 150℃ is better than slowly cooled, which in turn is better than unannealed one. At temperatures 200℃, 250℃ and 350℃, dark J-V plots for quenched electrodes are better or similar to slowly cooled

electrodes. Figure (3.23) shows that the dark J-V plot quality was in the order: 200℃ > 250℃ > 300℃ > 350℃ > 150℃ > 100℃ > unannealed.

b) Photo J-V Plots for MnP/polysolixane Coated CdSe Electrodes:

Figures (3. 24-3.28) show that photo J–V plots measured for MnP/polysiloxane-coated SC electrodes were improved by preannealing compared to untreated electrodes. Significant J-V plot enhancement was observed by annealing. Treated electrodes are better than the untreated ones as observed from J-V plot shape, fill factor and value of short circuit current. In addition to photocurrent J-V enhancement by coating with MnP/polysiloxane, further enhancement can be achieved by preannealing the CdSe thin films. Figures (3.24) through (3.28) indicate that preannealing of CdSe film electrodes followed by MnP/polysiloxane polymer coating, significantly enhances photo J-V plots. Moreover, cooling rate of preannealed CdSe, affects photo J-V plots for MnP/polysiloxane coated electrodes. Figures (3.24) through (3.28) summarize these findings.

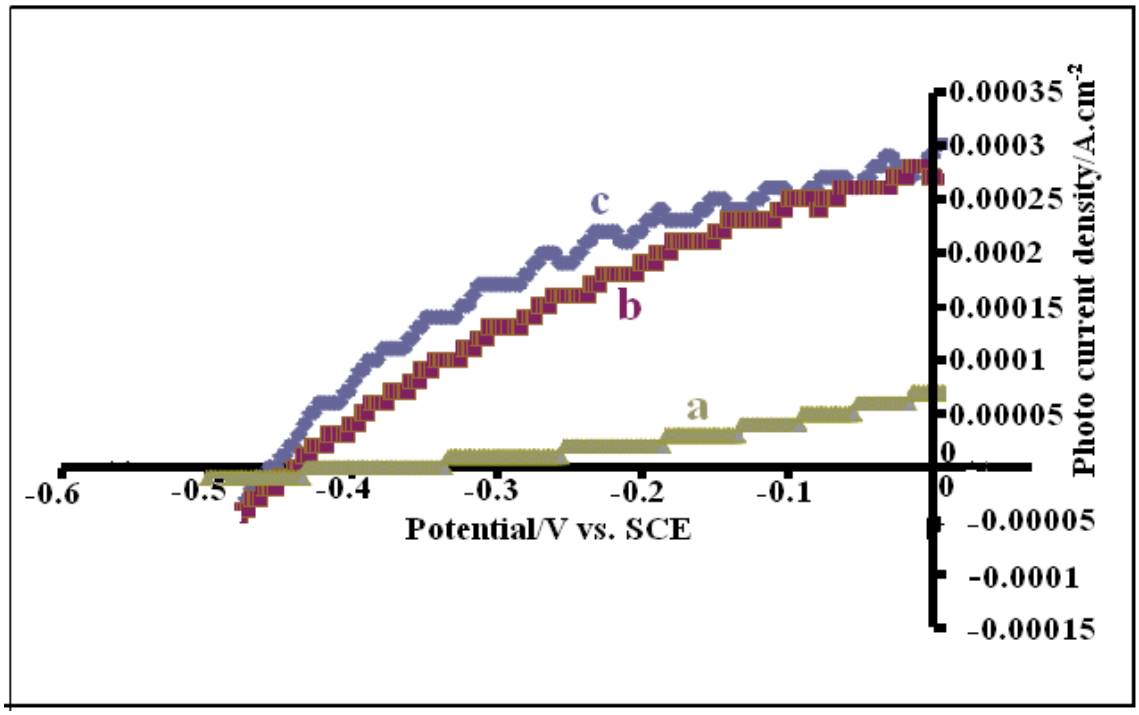

Figure (3.24): Photo J-V plots for MnP/polysiloxe coated CdSe electrodes, (a) unannealed,the others are annealed at 150^0 C , (b) slowly cooled and (c) quenched .

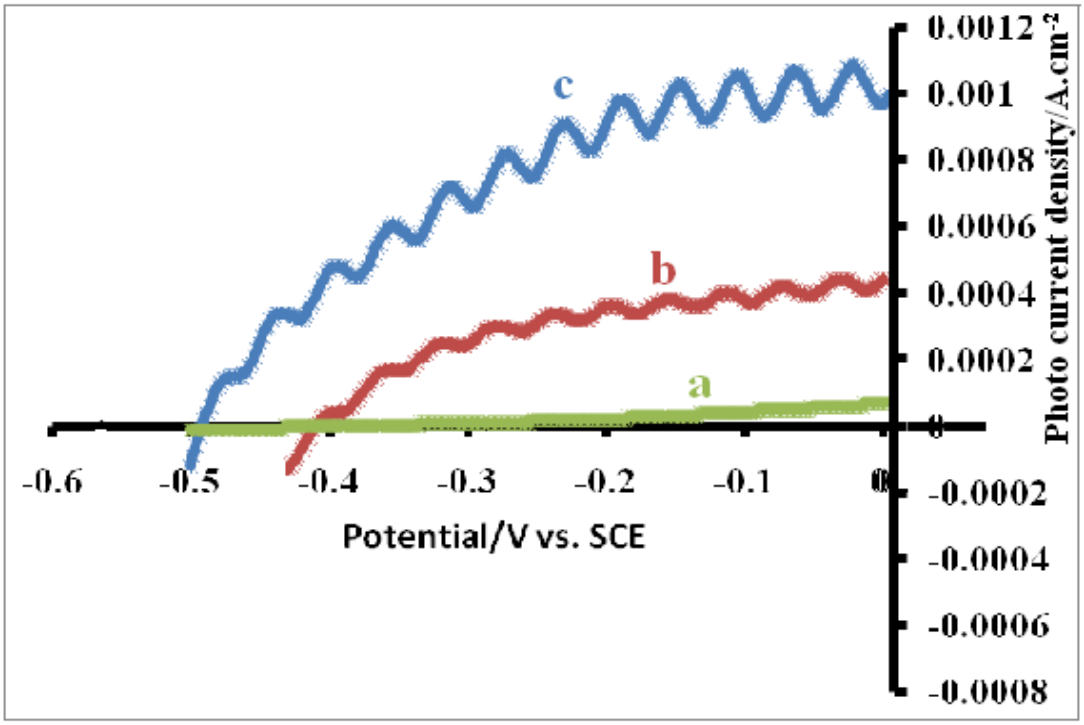

Figure (3.25): Photo J-V plots for MnP/polysiloxane coated CdSe electrodes (a) unannealed, the others are annealed at 200^0 C, (b) slowly cooled (c) quenched.

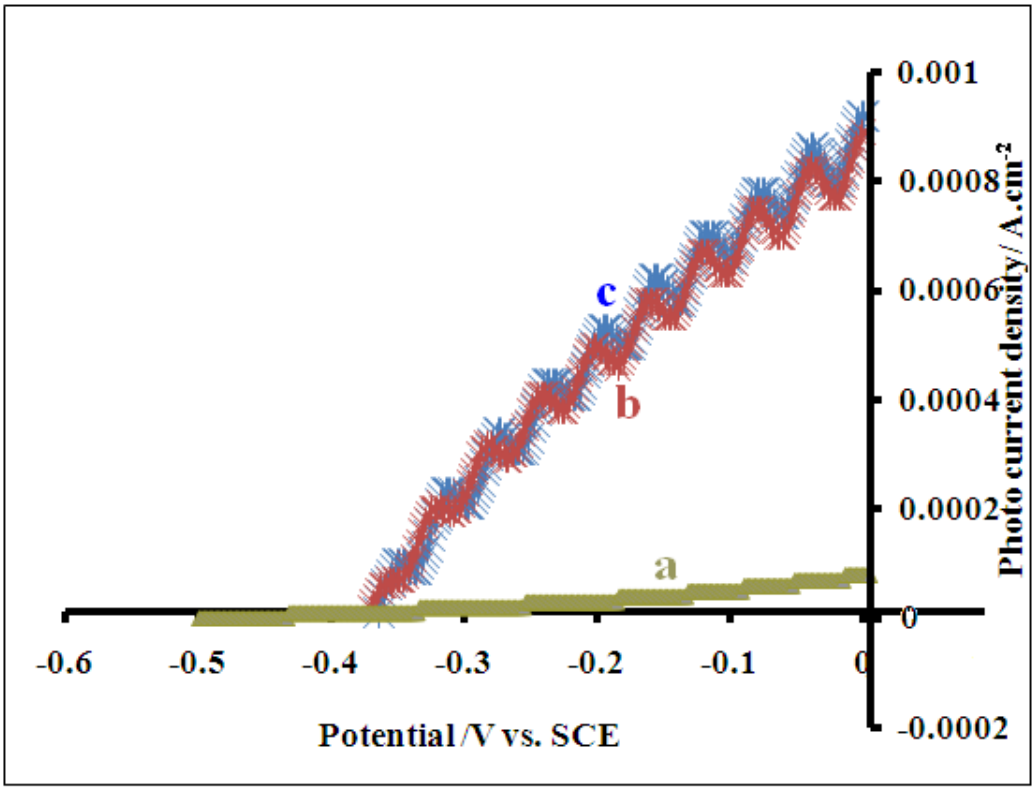

Figure (3.26): Photo J-V plots for MnP/polysiloxane coated CdSe electrodes, (a) unannealed, the others are annealed at 250^{0}C. (b) slowly cooled, (c) Quenched.

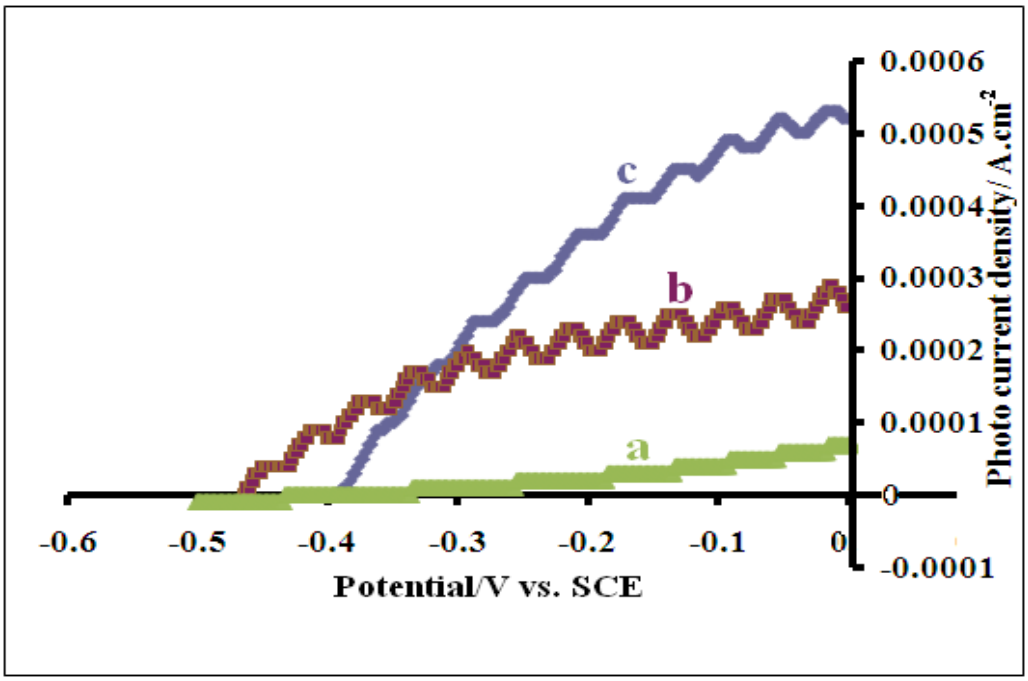

Figure (3.27): Photo J-V plots for MnP/polysiloxane coated CdSe electrodes (a) unannealed, the others are annealed to 300 ^{0}C, , (b) slowly cooled, (c) quenched.

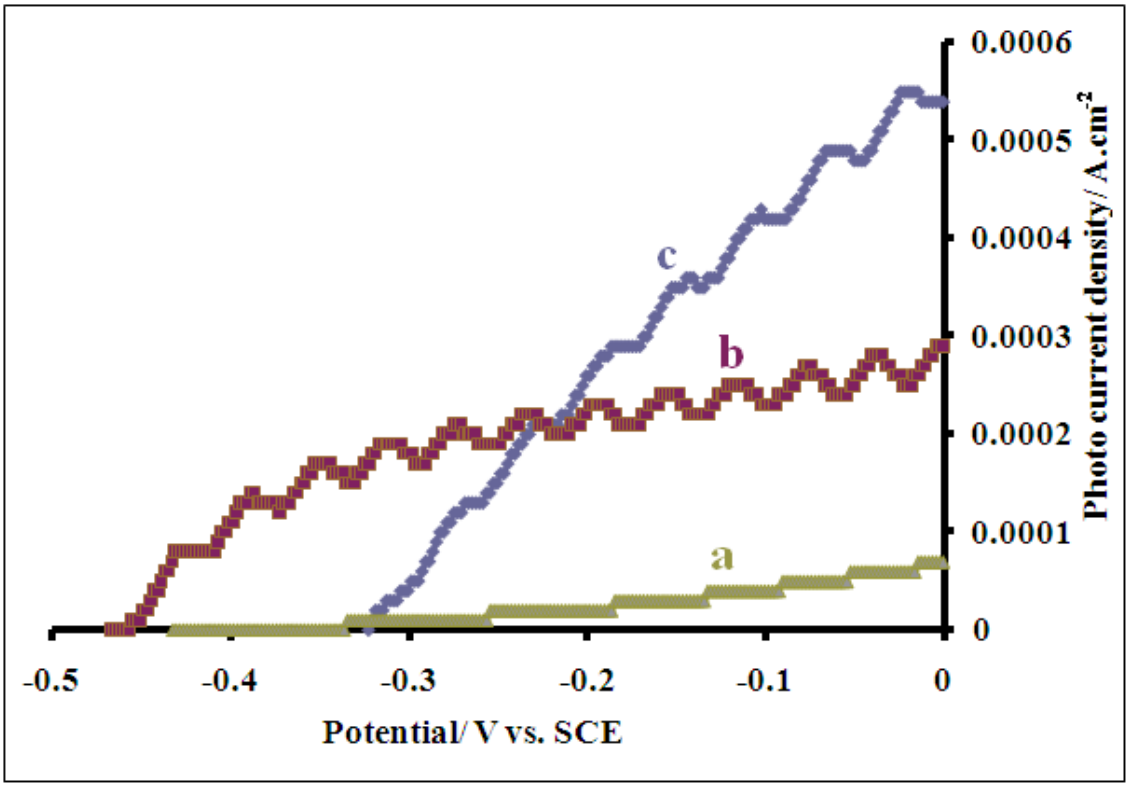

Figure (3.28): Photo JV plots for MnP/polysiloxane coated CdSe electrodes (a) unannealed, the others are annealed at 350^0C b) slowly cooled, (c) quenched.

In Figure (3.25), the electrode quenched from 200^0C gives the best efficiency in comparison with other electrodes. Figure (3.25) shows that the electrode quenched from 200^0C is better than the slowly cooled electrode. Figures (3.24-28) also show that quenched electrodes have better or similar photo J-V plots than slowly cooled counter parts. Among the CdSe electrodes, coated with MnP/polysiloxane, prequenched from different temperatures, the photo J-V plot quality was in the order: 200^0C > 250^0C > 300^0C > 350^0C >150^0C > unannealed.

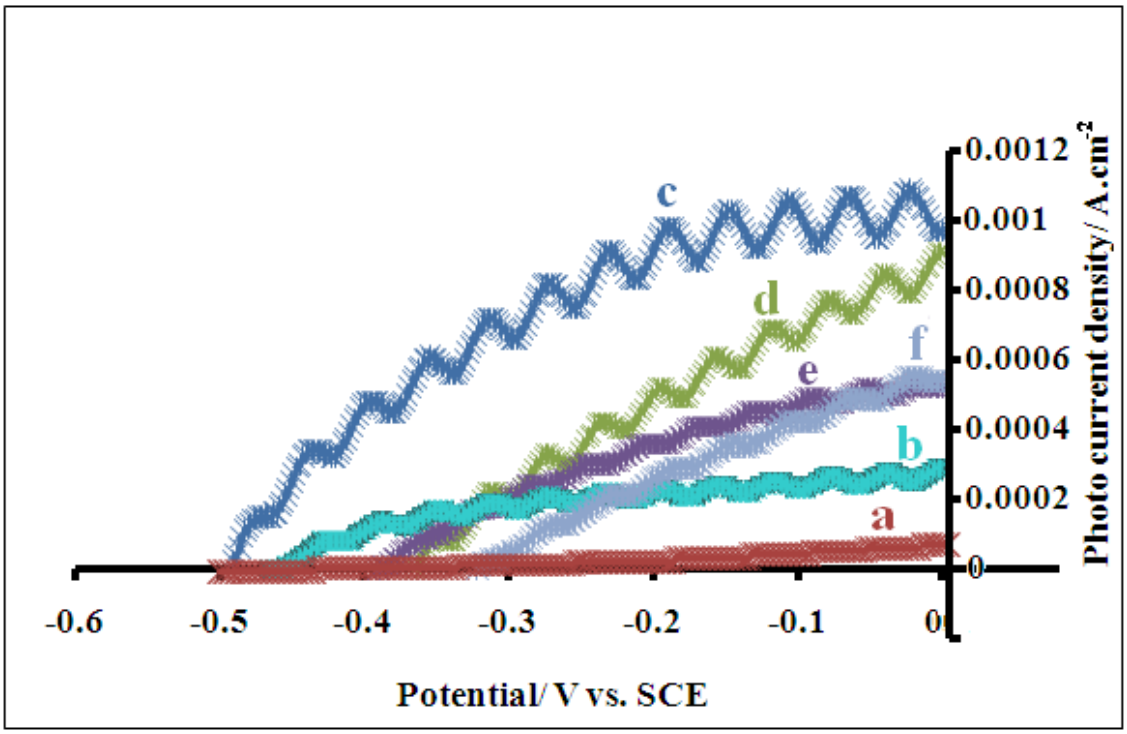

Figure (3.29): Photo J-V plots for MnP/polysiloxane coated CdSe electrodes quenched from (a) unannealed, (b) 150^{0}C, (c) 200^{0}C (d) 250^{0}C, (e) 300^{0}C (f) 350^{0}C.

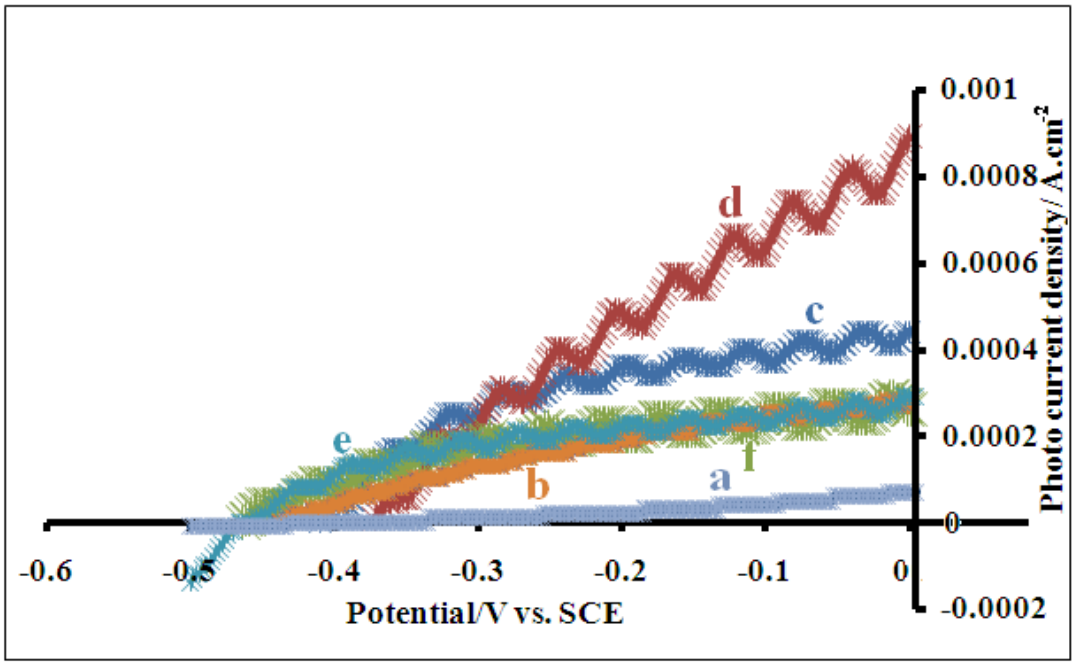

Figure (3.30): Photo J-V plots for MnP/polysiloxane coated CdSe electrodes slowly cooled from: (a) unannealed, (b) 150^{0}C, (c) 200^{0}C, (d) 250^{0}C, (e) 300^{0}C, (f) 350 ℃.

Coating with MnP/polysiloxane, protected the CdSe film from peeling out. Figure (3.31) shows pictures of different films after exposure to PEC conditions.

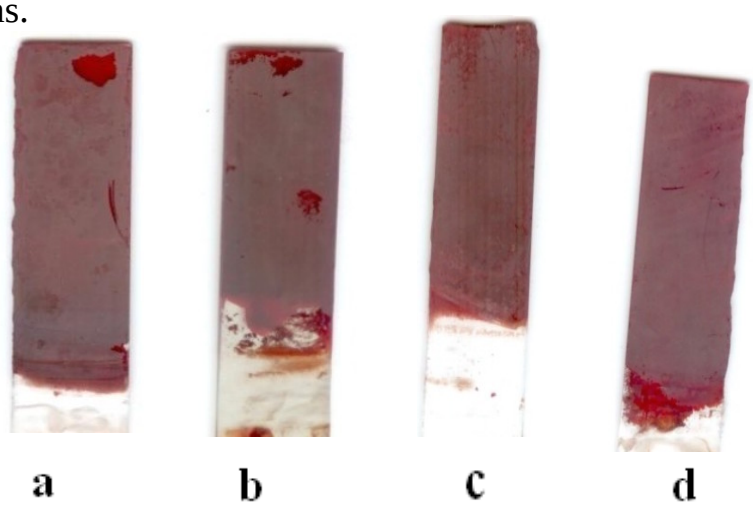

Figure (3.31): Some electrodes after coating MnP/polysiloxane, and after using in PEC. a) Pre-Annealed at 150℃, b) Annealed at 200℃, c) Annealed at 250℃, d) Annealed at 300℃.

Comparing coated electrodes in Figure (3.31) with that in Figure (3.15), we see that the coated ones are not broken down in the redox couple.

c) Electrode Stability

The stability of the MnP/polysiloxane coated CdSe electrode, under PEC conditions, was studied. Values of short circuit current density (J_{sc}) were measured over a range of periods of time, while keeping the electrode under steady illumination ($0.0212 Wcm^{-2}$) and under a 0.00 V bias vs. SCE. Plots of values of J_{sc} vs. time were constructed as shown in Figures (3.32-34).

d) Effect of Annealing on Electrode Stability:

Effect of preannealing on MnP/polysiloxane covered CdSe film stability has been studied using redox couple which is 0.1 M of (S, Na_2S, KOH) under illumination. Plots of $I_{s.c}$ vs. time have been constructed for untreated electrodes and pre-heated/pre-cooled ones from 250^0C using slow and rapid cooling. Figures (3.32-34) show these results. In each plot, the $J_{s.c}$ starts with very small values, and increases with time until a steady value was reached. This demonstrate the stability of CdSe thin films under PEC conditions for as long as 250 min. It is clear that the pre-heated electrodes gave higher $J_{s.c}$ values than untreated ones. Figure (3.32) shows that the electrode pre-annealed at 250℃ has better $J_{s.c}$ value than unheated one.

Figure (3.33) shows that electrodes annealed at 200℃ have better $J_{s.c.}$values that the un annealed one. Figure (3.34) shows that quenched electrode from 150℃ has better values than the slowly cooled one. Among different temperatures used, the 200℃ was the optimal annealing temperature. For quenched samples, values of $J_{s.c}$ varied in the order: 200℃ > 250℃ > 150℃ > un annealed.

e) Effect of Rate of Cooling on Electrode Stability:

Effect of cooling rate on stability of MnP/polysiloxane coated CdSe electrodes under PEC conditions was studied. Figures (3.32-34)

show that samples quenched from 250℃, 200℃ and 150℃ have better values than the un-treated ones.

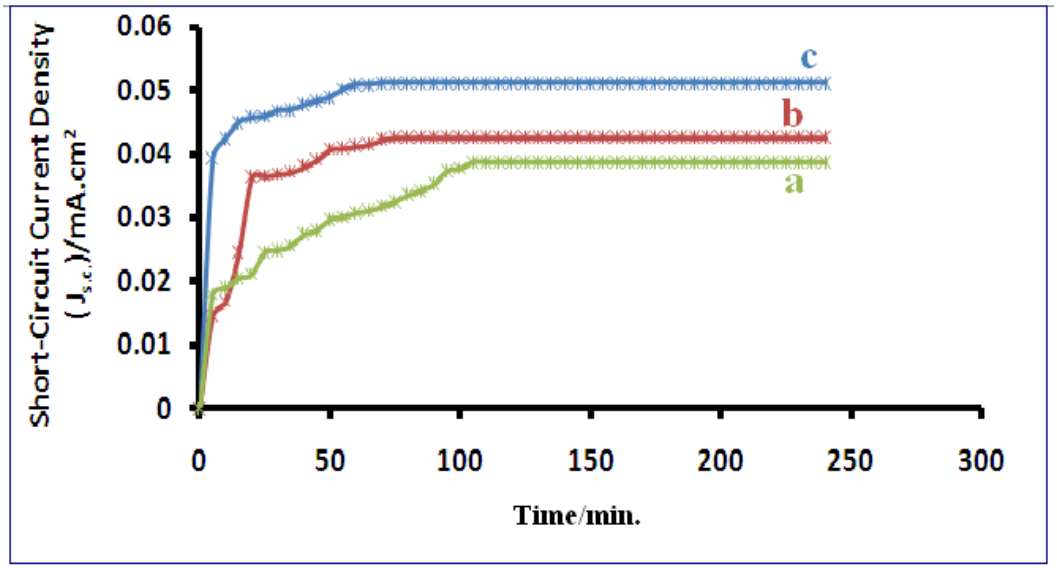

Figure(3.32): Short circuit current density vs. time measured for MnP/polysiloxane coated CdSe thin film electrodes, (a) unannealed, the others are annealed at 250^0C, (b) slowly cooled, (c) quenched.

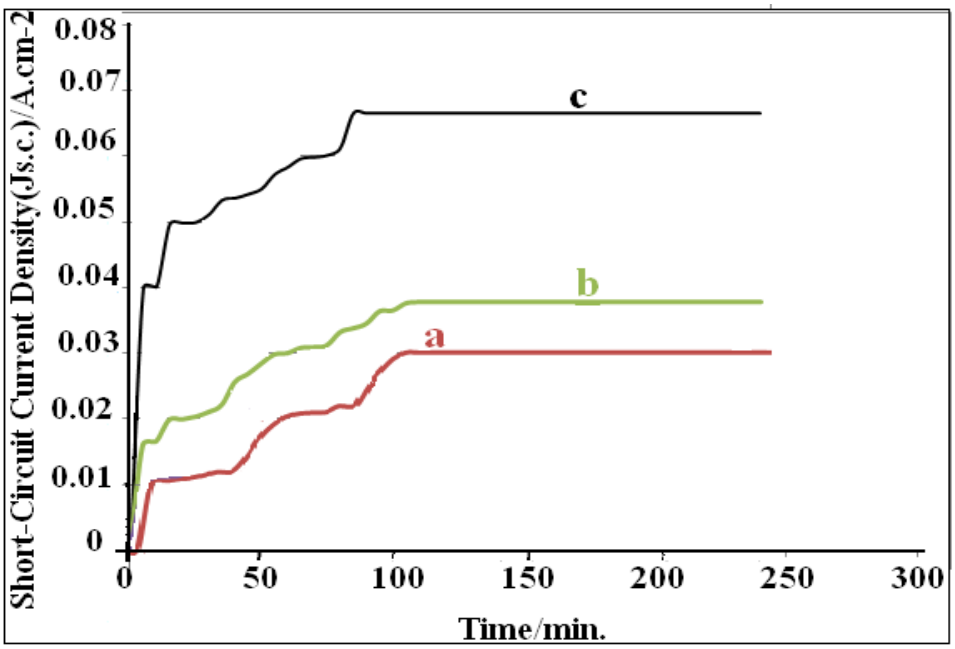

Figure (3.33): Short circuit current density vs. time measured for MnP/polysiloxane coated CdSe thin film electrodes, (a) unannealed, the others are annealed at 200^0C, (b) slowly cooled, (c) quenched.

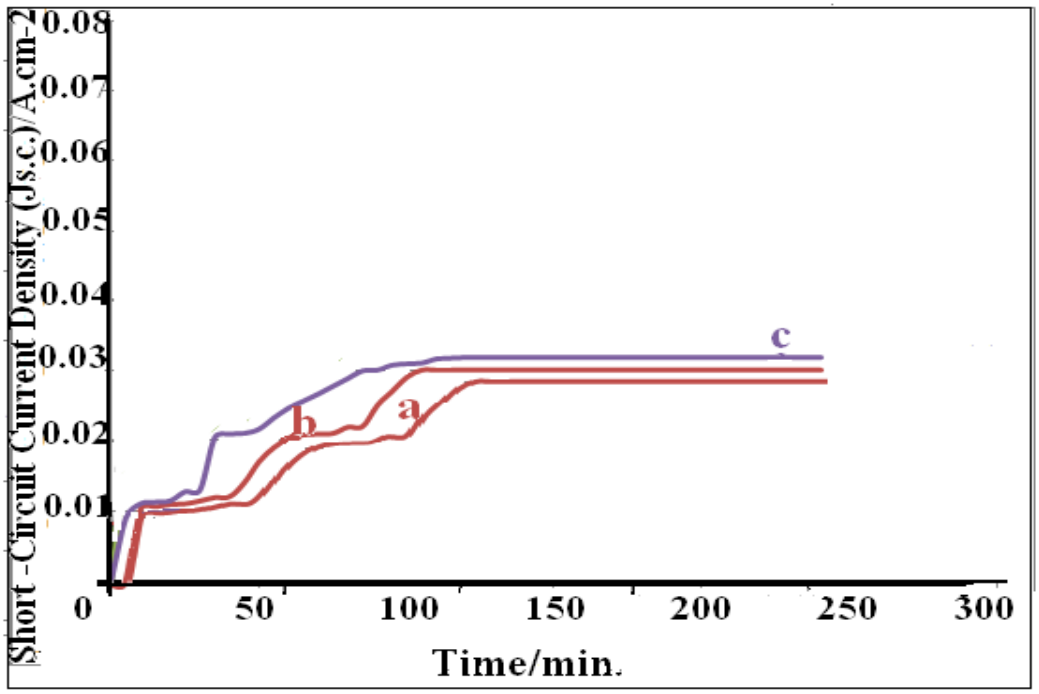

Figure (3.34): Short circuit current density vs. time measured for MnP/polysiloxane coated CdSe thin film electrodes, (a) unannealed, annealed at 150^0C, (b) slowly cooled, (c) quenched.

Figure (3.33 a and b) shows that the electrode quenched from 200^0C (3.33-a) has higher $J_{s.c.}$ values than slowly cooled electrode. This result is consistent with previous results. Figure (3.34 a and b) shows similar result for 150 ℃. The CdSe thin film quenched from 200℃ gives the best value, followed by the one quenched from 250℃ , and the one quenched from 150℃,the slow cooled sample from 250℃ respectively.

f) Cell Efficiency Studies:

MnP/polysiloxane modification of CdSe thin films enhances the light-to-electricity conversion efficiency. Table (3.3) shows the data of Efficiency (ή), open circuit potential ($V_{o.c.}$), short circuit current density

($J_{s.c.}$) and fill factor (FF%) for different electrodes. The Table shows the different PEC characteristics for pre-heated electrodes are higher than for non-heated ones. The Table also shows that the $J_{s.c.}$ and efficiency values for quenched electrodes are higher than those for slowly cooled ones, except for electrode heated at 250℃ which has the same values for quenched and slowly cooled ones. The best value of efficiency is that for electrode quenched from 200℃. For slowly cooled ones the best efficiency is for 250℃, but the quenched value for 200℃ is still higher.

Open circuit potential and fill factor for slowly cooled electrodes are higher than or equal for quenched electrodes, as shown in Table (3.3).

Among different electrodes, the slowly cooled electrode from 200℃ showed highest FF value.

Table (3.3): Values of efficiency (ή), open circuit voltage ($V_{o.c.}$), current density($J_{s.c.}$) and for fill factor (FF) for MnP/polysiloxane coated CdSe film.

Entry Number	Annealing* ^0C Temperature	Cooling Rate	Vo.c. V	Js.c. mA/cm^2	** ή%	*** FF %
1	Room Temp.	—	-0.34	0.1	0.07	42
2	150	Quenched	-0.46	0.3	0.26	39
3		Slow	-0.44	0.28	0.21	37
4	200	Quenched	-0.5	1	1.06	45
5		Slow	-0.42	0.4	0.43	54
6	250	Quenched	-0.38	0.9	0.59	36
7		Slow	-0.38	0.9	0.59	36
8	300	Quenched	-0.36	0.52	0.36	40
9		Slow	-0.47	0.25	0.26	48
10	350	Quenched	-0.32	0.53	0.28	35
11		Slow	-0.46	0.29	0.27	44

*All measurements were conducted in aqueous (KOH, S, H_2S) at 25°C.

**ή (%)=[(maximum observed power)/(reach- in power)]×100%.

***FF=[(maximum observed power)/$I_{s.c.}\times V_{o.c.}$] ×100%.

Chapter Four

Discussion

4.1 Introduction

Structural properties of CdSe thin films were studied by X-ray diffraction [83]. CdSe can form hexagonal wurzite-type structure or cubic, zinc blend –type structure. XRD pattern revealed that the films are polycrystalline in nature with hexagonal phase.

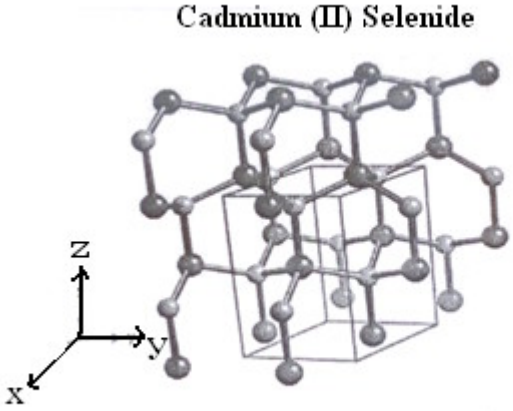

Figure (4.1): Wurtzite sructure of CdSe [84]

The films prepared by CBD are usually composed of closely spaced nanocrystals [85]. The band gap engineering of films is possible by controlling the nanocrystals size, which can be done by changing the parameters of deposition [86-87]. To deposit a film, it is necessary to slow down the rate of chemical reactions to such an extent that CdSe is either directly formed on the substrate or small particles of CdSe are formed in the solution and subsequently adhere to the growing film, rather than

aggregate into larger particles in the solution and precipitate out. In CBD, this rate control is accomplished by a slow generation of Se^{-2} ions in the deposition (e.g., by alkaline hydrolysis of sodium selenosulphite (Na_2SeSO_3) [88]. Some authors distinguish between two regimes for the formation of CdSe films. One by ion deposition mechanism, where CdSe is grown by ionic reaction between Cd^{+2} and Se^{-2}, while, the other by cluster deposition mechanism, where CdSe is formed by conversion of $Cd(OH)_2$ in the deposition solution by selenide ion. Both mechanisms may in principle occur currently. Their relative importance is affected by the concentration in the deposition solution, the solution pH, temperature, etc [89]. This leads to a large number of free parameters that can be adjusted in the procedure of CBD. The deposition parameters are usually optimized to obtain secularly reflecting films with good adherence to the substrate [90-92]. By changing the deposition parameters, one can control the size of nanocrystals and consequently the band gap energy of the film. This opens a range of application possibilities. The influence of light illumination of solution during chemical deposition of CdSe NC's was observed by Hodes [93].

4.2 Effect of Annealing and Rate of Cooling on Electronic Absorption Spectra

In Figures (3.1-3.4), annealed electrodes at 100 ^{0}C and 200^{0}C have better values than the un annealed electrode. The unannealed electrode has better value than the electrode heated at 350^{0}C. Quenched electrodes have better values than slowly cooled ones. Annealed electrode at 200^{0}C, has the best spectra for quenching and slow cooling samples. This is due to surface enhancement of CdSe thin films. Table (3.1) shows the variation of the band gap "E_g". As the annealing temperature was increased, the crystallite size of CdSe thin film was increased resulting in narrower band gap. This is seen in Tables (3.1) and (3.2)[94]. Therefore, annealing the films exhibits strong red shift in their optical spectra due to localization of charges in individual nanocrystals. There is no significant change in band gap due to structural phase transform of CdSe from metastable cubic to stable hexagonal, as previous workers reported [95]. The shift in E_g (~0.3eV) and the variation of grain size of CdSe crystallite from 30A^0 to 40A^0 has been observed when the temperature of the bath varies from 26^{0}C to 80^{0}C. These changes are attributed to the quantum size effect in nanocrystalline semiconducting films. CdSe is not stable, there is no need to heat it at high temperatures [96].

4.3 Effect of Annealing on Photoluminescence Spectra

We used optical absorption and photoluminescence (PL) spectroscopy to characterize the films. The typical absorption and PL spectra are demonstrated in Figures (3.5-3.6).

a) Quenched CdSe Electrodes

Figure (3.5) shows that there are differences in the spectra, depending on the annealing temperature. The best value is for 200^0C, which parallels of electronic absorption spectra and J-V plots for both photo and dark current. There is no significant change in band gap due to structural phase transform of CdSe from metastable cubic to stable hexagonal, as previous workers reported [97].

b) Slowly Cooled CdSe Electrodes

Figure (3.6) indicates that slow cooling depends on annealing temperature. The best value is for 200^0C then for 350^0C. No great difference between slow cooling from 100^0C and un annealed electrode was observed. This indicates that highest enhancement occurs by annealing at 200^0C. At higher temperatures, some damage may occur at the film, by oxidization or increased imperfection [98].

4.4 Effect of Coating Thin Films with a Layer of Polymer

In Figures (3.9-3.14), both dark J-V plots and photo J-V plots were poor. No difference appears between dark and photo J-V plots, the reason was the damage that occurred to the wafer layer in the redox couple solution. Pictures of the damaged wafers are shown in Figure (3.15). When the redox couple was changed, and a solution of 0.1M of [Na_2S, S , KOH] was used, the same poor behavior was obtained as shown in Figures (3.13-3.14). For enhancement of the J-V plots, an electrode was treated carefully with smooth glass papers after etching process prior to thin film deposition. The layer was a little quite well adherent to the substrate, as shown in Figure (3.16). For a better enhancement the electrodes were covered by a layer of MnP/polysiloxane matrix as shown in Figure (2.9). In this study the effects of preannealing, rate of cooling, and MnP/polysiloxane modification on electrode stability and efficiency were studied. Consistent with earlier reports [99-100] preannealing of SC wafers enhanced the photocurrent and dark current J–V plots. Cooling rates of the preheated wafers also affected the J–V plots. Modification with MnP/polysiloxane improved the J–V plots, efficiency and stability of CdSe electrodes. Combining the three processes of heating, cooling rate and MnP modification showed rather remarkable enhancement in electrode efficiency. The effects of SC wafer

preheating and of cooling rate on quality of dark and photo J-V plots have been demonstrated in earlier reports [101-102]. Preheating and cooling rate processes affect the efficiency of CdSe electrode and its J-V plots. Quenching showed higher efficiency than slow cooling. Preheating and cooling rate of CdSe wafers improves the crystal in many ways. Surface roughness and crystal defects are lowered by treatment [103-110]. Such improvements in crystal quality would yield enhancement in electrode J–V plots and efficiency. Modification with MnP/polysiloxane matrices further enhanced the CdSe electrode efficiency under PEC conditions. Earlier work indicated enhancement in dark and photo J–V plots by coating with MnP/polysiloxane matrices on single crystals of GeAs. Consequently, enhancing the electrode conversion efficiency [111-116]. The MnP behaves as a charge–transfer catalyst between the SC surface and the solution redox couple. This process would thus enhance the current across the solid/liquid interface. It also speeds up the release of holes from the SC valence band edge [117-118]. Combining the three techniques together gives the best results in terms of J–V plot quality, electrode stability and efficiency. Table (3.3) indicates that electrodes coated with MnP, after preheating and quenching from 200 ◦C gives the best conversion efficiency (∼1.06%). Preheating and quenching enhance the SC wafer in terms of crystal quality,

defect reduction and surface roughness exclusion. MnP behaves as additional redox couple that acts as charge–transfer catalyst to speed up release of holes from valence band and protect the SC surface from photo degradation, and less recombination rate.

4.5 Effect of Annealing on CdSe Film Characteristics

Annealing of SC wafers is reported to enhance their characteristics, such as crystal structure, and optical absorption increases with increase in annealing temperatures. This may be due to increase in crystalline size, decrease in defects and change in color from red –orange, to dark brown. Literature reported that room temperature electrical resistivity for CdSe thin films ($3.25\times10^{5}\Omega$.cm) decreased to ($1.17\times10^{3}\Omega$.cm) after annealing to temperature 673 K [119]. The decrease in resistivity after annealing is due to increase in crystalline size of CdSe thin films, and better sintering between crystallites. This is in turn increase electron mobility as will be described.

4.5.1 Effect of Annealing on Dark J-V Plots

When J-V plots were measured in dark, for annealed and un annealed electrodes, better values were obtained for annealed ones. The degree of improvement depends on the annealing temperature and on rate of cooling. The samples annealed at 200^{0}C have better J-V plots.

Figures (3.17-3.22) indicate that J-V plots are improved by annealing at 350, 300, 250, 200, 150, 100 ^{0}C. The enhancement in dark J-V plots is due to increase in grain size and enhancement of film structure by annealing. The carrier mobility is enhanced within the crystallite. The heat treatment increases the adherence of the films to their substrates. Annealing eliminates disorder in crystallites. Moreover, sintering between different crystallites is improved by annealing. These effects combined give higher carrier mobility within the thin film.

4.5.2 Effect of Annealing on Photo J-V Plots

Figures (3.24-3.28) show that annealing CdSe thin films improves the photo J-V plots. The degree of enhancement depends on the degree of annealing temperature and on the cooling rate. The effect of annealing is better for 200^{0}C and 250^{0}C. Quenched and slowly cooled samples from 200, 250 ^{0}C give better photo J-V plots than other samples. Annealing of CdSe samples improves crystallite quality of the films by removing random strain, and consequently decreasing resistivity and reducing surface states. For temperatures above 250^{0}C, the enhancement of the films was found to decrease as shown in Figure (3.29). This could be due to high oxidization ratio of nanoparticles. Increase of imperfections may also occur. Consequently resistance of FTO/ glass may also increase at high

temperatures.

4.5.3 Effect of Annealing on Film Stability

Plots of J_{sc} vs time have better values for annealed samples than untreated ones. Preheating enhances the J_{sc} values. As mentioned previously, the heating process enhances the surface of the sample, so it improves the stability of thin films. This is due to increased size and removal of defects in the deposited films as shown in Figures (3.32-3.34). In addition, there is an increase in minority carrier diffusion to electrolyte solution in PEC.

4.6 Effect of Cooling Rate on CdSe Film PEC Characteristics

a) Dark J-V Plots

As in Figures (3.17-3.22), the quenched samples have better J-V plots than slow cooled ones. Samples annealed at 200^0C are the best. Quenching improves the composition and the surface of the sample. By cooling, metastable atoms try to move again to their stable positions. No great difference noticed between slow cooling and quenching processes. This is due to improvement of CdSe film crystallinity, and therefore enhancement of dark current density.

b) Photo J-V Plots:

Figures (3.24-3.28) show that quenched samples have better J-V plots than

slowly cooled. The best J-V plot is for a quenched sample from 200^0C. No great difference is noticed between the quenched J-V plots and the slow cooled ones, at any of the annealing temperatures.

c) Film Stability

Figures (3.32-3.34) indicate that $J_{s.c.}$ vs. time plots are better for quenched electrodes. The best J_{sc} value was observed for the sample quenched from 200^0C. Quenching enhances the film surface and improves the stability of the electrodes.

4.7 Effect of Cooling Rate on Cell Efficiency

Cooling rate affected the CdSe electrode conversion efficiency. Preheating enhanced electrode efficiency. Quenching CdSe thin films from 150℃, 200℃, 250℃, 300℃ and 350℃ shows better efficiency and higher fill factor than slow cooling. The values of fill factor and conversion efficiency, are better for quenched electrodes than for slowly cooled ones, as shown in Table (3.3). Quenched electrode from 200℃ has the best conversion efficiency (1.06%) compared to the slowly cooled one which is (0.43%). Thus quenching of heated CdSe thin films improves their crystallinity by affecting their dislocation density and structural defect concentration.

Conclusions

1) Thin films of CdSe onto FTO/glass substrates have been prepared by CBD for the first time.

2) The CdSe thin films showed enhancement in their electronic absorption and photoluminescence spectra by annealing and controlled cooling rate.

3) The naked CdSe films did not exhibit useful PEC behaviors.

4) Roughing FTO surface, prior to CdSe deposition slightly enhanced its PEC characteristics.

5) Coating the CdSe films with metalloporphyrine (Mn^{II}/Mn^{III} P) ions, imbedded inside polysiloxane matrices, significantly enhanced their PEC characteristics {open circuit voltage $V_{o.c.,}$ short circuit current density $J_{s.c.}$, fill factor FF, efficiency and stability }

6) Preannealing of CdSe, electrodes followed by MnP/polysiloxane coating gave further enhancement in their PEC characteristics.

7) Cooling rate of preannealed CdSe electrodes with MnP/polysiloxane affected their PEC characteristics.

Suggestions for Future Works

For future work, we recommend doing the following:

1) Use preheating and rate of cooling techniques to improve other thin films as CdZnSe.

2) Prepare CdSe thin films by other techniques such as electro deposition, and modify them as described here.

3) Try to coat the CdSe wafers by other types of polymers and electroactive species.

4) Study the rate of cooling on CdSe thin films prepared at low temperatures.

5) Study the effect of light intensity and dark on the chemical bath solution and their effects quality of thin films.

References

[1] M. Lacascico, "*Application of Semiconductor Nanocrystals to Photovoltaic Energy Conversion Devices",* **www.evident.com.** Aug. (2002).

[2] E. Norvell, "*Cadmium Selenide Semiconducting Nanorods Vertically Aligned to Conductive Substrate for Solar Cell Application",* **California Polytechnic State University**, San UIS obi spo.

[3] Y. Anderson, *" Semiconductor-Electrolyte PV Cells employing CdSe and CdTe "***Anderson Y.G. L.B.** 8 Sep. (2005).

[4] Y. G. Chai, "*Single Crystal CdSe Solar Cell"*, **Electron Devices, IEEE Transactions** on , (1977) Volume 24 P. 492-496.

[5] S. Cimen, *"Solar Materials*",**www. no slab. Boun.edu.tr./solar cell.pdf,** (2005).

[6] Boyd. "*Quantum dot recipe may lead to cheaper Solar Panels*", **Rice University**, (2007), 348-678 rice University.

[7] M. Simurda a, P. Nemec, P. Formanek, I. Nemec c, Y. Neˇmcova, P. Maly, "*Morphology of CdSe films prepared by chemical bath deposition: The role of substrate"*. **Thin Solid Films** 511 – 512 (2006), p 71 – 75

[8] M. Behboudnia and Y. Azizianekalandaragh, "*Synthesis and characterization of CdSe semiconductor nanoparticles by ultrasonic irradiation*", **Materials Science and Engineering**: B, Volume 138, March 2007, Pages 65-68.

[9] S.S. Kale, C.D. Lokhande, "*Thickness-dependent properties of chemically deposited CdSe thin films"*. **Materials Chemistry and Physics** 62 (2000).

[10] C. Vargas-Hern ndez*, V. C. Lara, J. E. Vallejo, J. F. Jurado, and O. Giraldo, " *XPS, SEM and XRD investigations of CdSe films prepared by chemical bath deposition*", **phys. stat. sol. No. 9**, 1897–1901 (2005).

[11] C.D. Lokhande1, Eun-Ho Lee, Kwang-Deog Jung, Oh-Shim Joo, *"Ammonia-free chemical bath method for deposition of microcrystalline cadmium selenide films*", **Materials Chemistry and Physics** 91 (2005) 200–204.

[12] E. Lifshitz , I. Dag, I. Litvin, G. Hodes, S. Gorer, R. Reisfeld, M. Zelner, H. Minti, "*Optical properties of CdSe nanoparticle films prepared by chemical deposition and sol–gel methods",* **Chemical Physics Letters** 288_1998.188–196.

[13] Q. Dai, Y. Song, D. Li, H. Chen, S. Kan, B. Zou, Y. Wang, Y. Deng, Y. Hou, S. Yu, L. Chen, B. Liu, G. Zou," *Temperature dependence of band gap in CdSe nanocrystals. This function is practically applicable to any particle size and temperature*", **Chemical Physics Letters** 439 (2007) 65–68.

[14] H. Y. Si, Z. H. Sun, H. L. Zhang**.** "*Photoelectrochemical response from CdSe-sensitized anodic oxidation TiO2 nanotubes".* **Colloids and Surfaces A: Physicochem. Eng.** Aspects xxx (2007).

[15] M. E. Van Hulle, " *Space charge region in thin AgBr films"* ,**Surface Science,** Volume 58, 1976, p 605- 608.

[16] L.Hollman, J. P. Hallais and J. C. Price, in "*Current Topics in Materials and Science",* E. Kaldis, **North Holland Publ. Co.** Vol.5, ed. (1980), p. 1.

[17] A. Floyd, "*Electronic Devices*", **Electronic Devices Fourth Edition**, pp 78-90.

[18] K. W. Frese, Jr., in *"Semiconductor Electrodes*", **ed. H. Finklea, Elsevier, Amsterdam**, (1988), p. 373.

[19] K. S. V. Santhanam, in "*Photoelectrochemical Solar Cells*", ed. **KS. V. Santhanam and M. Sharon, Elsevier, Amsterdam, Oxford, N. Y. Tokyo,** (1988), pp. 1-14.

[20] K. Rajesh war, p. Singh, and j. DuBow, *"Energy conversion in photoelectrochemical system-a review",* **Electrochim.Acta,**23 (1978)1118**.**

[21] P. Calza, C. Minero, A. Hiskia, E. Papacostantinou and E. Pelizzetti, *"Photolytic and photo catalytic deco potion of promomethanes in irradiated aqueous solutions*", **Appl. Catal.** B, 21 (1999) 191- 202.

[22] S. Chandra, in "*Photoelectrochemical Solar Cells ",* **Gordon and Breach Science Publishers**, New York, (1986), pp. 88-103.

[23] See ref. [17] p.99.

[24] S., Searles, D. L. Pulfreu, "*analysis of SCR recombination*", **Trans. Electron Devices (USA)**, Volume 41, Number 4,in HBT's P. 476-833 (1994).

[25] **http://www.eia.doe.gov./kids/energyfacts/sources/renewable /solar.html,** 12/4/2008.

[26] See ref. [17] p.81-82.

[27] M. Graetzel, *"Photovoltaics Quantum dots promise next-generation Solar Cells"*, **Nature414**, (2001), 338.

[28] **http://en. Wikipedia./wiki/photovoltaics,** 12/4/2008.

[29] **http://www.absak. Com/basic/solar power html**, 12/4/2008.

[30] K. Rajesh war, p. Singh, and J. DuBow, *"Energy conversion in Photoelectrochemical systems- a review"*, **Electrochim. Acta**, 23 (1978) 1118.

[31] A. J. Nozik, "*Photo electrochemistry":* **Application to Solar Energy Conversion**, 29 (1978) p (189-192).

[32] B. Finnstr m, in "*Solar Energy –Photochemical Processes Available for Energy Conversion*", vol. 14, eds. S. Clae ssonand B. Holmstr m, National Swedish. **Board for Energy Source Development** (1982), p. (56-64).

[33] H. O. Fink lea, in "*Semiconductor Electrodes",* **ed., Elsevier, Amsterdam**, (1988), p. 10.

[34] See ref. [33], pp.18-22.

[35] See ref., [33], p. 7.

[36] H. Gerischerm,"*Photovoltaic and Photo electrochemistry Solar Energy Conversion"*. **Ed., F. Cordon, W. P. Gomes, and W. Dekeyser, Plenum Publishing Corporation, New York**, (1980), pp. 246-253.

[37] V. Aroutiounian, S. Petrosyanand A. Khachatryan, "***Solar Energy*" Materials and Solar Cells** Volume 89, (2005), Pages 165-173.

[38] R. Memming, in "*Comprehensive Treating of Electrochemistry"*,Vol.7, **eds. B. E. Conway, et al., Plenum Publishing Corporation, New York**, (1983), pp. 540-544.

[39] H. Tachikawa, L. R. Faulker, in "*Laboratory Technique in Electro analytical Chemistry"*, **eds. P. T. Kissinger and W. R. Heinemann, Markel Dekker, Inc., New York**, (1984) pp. 647-648.

[40] See ref. [32] pp. 67-70.

[41] H. Gerischerm, "*The rule of semiconductor structure and surface properties in photoelectrochemical processes"* ,J**. Electronical Chem**., 150 (1983) 553-569.

[42] See ref. [32] pp. 32-38.

[43] S. M. Sze, "*Physics of Semiconductor Devices*", **John Wiley and Sons, Inc. New York**, (1981), pp. 380.

[44] A. J. Nozik. In " *Photovoltaic and photoelectrochemical Solar Energy Conversion"*, **eds. F. Cordon, W. P. Gomes, and W. Dekeyser, Plenum, Publishing Corporation, New York**, (1980), pp. 280-281.

[45] S. A. Rangel, *"Hydrogen Extended defect Interactions in Hetroepetaxial InP Materials and Devices",* **Solid State Electronics**, **41** (1997) p. 359-380.

[46] See ref. [43] p. 381.

[47] L. E. Katz, *"VISI Technology"*, **ed. S. M. Sze, McGraw Hill Book Company, New York,** (1983), pp. 154-156.

[48] N. S. Lewis, "*Frontier of Research in Electrochemical Solar Energy Conversion",* **J. electorally Chem.,** 508 (2001), p. 1-10.

[49] See ref.[4] p. 499.

[50] S. Berkekey, "*Nanocrystals CdSe Solar cell"*, **Research News, Berkekey Lab. Lyuu Yarris**, (5b), 20 oct.(2005).

[51] S. E. Shaheen, D. S. Ginley, and G. E. Jabbour, "*Organic-Based Photovoltaics: Toward Low-Cost Power Generation",* **MRS Bulletin**, **30**, (2005), p. 10.

[52] See ref. [30] p. 192-222.

[53] **http://en.wikipedia.org/wiki/Fick's_law_of_diffusion,** 5/7/2009.

[54] S. Soundeswaran, O.S. Kumar and R. Dhanasekaran,"*Effect of Ammonium Sulphate on CBD of CdS Thin Films"* **Materials Letters, 58** (2004) 2381-2385.

[55] A. Lukinskas, I Savickaja, "*Regularities of Electrochemical Formation of CdSe Films on Ti surface"*. **Dep. Of Met. Electrochemistry, Institute Chemistry, LT- 2600 Viluia, Lithuania.**

[56] G. Safra and O. Gesti, "*TEM study of CdSe prepared by the selenization of thin layers"*. **Research Institute for Technical Physics and Materials Science, HAS, Budapest, Hungary**, (2005).

[57] D. D. Eya, Ph. D. "*Optical Properties and Appl. Of CdSe Thin Films Prepared by CBD Technology"*. **The Pacific Journal of Science and Technology**, Volume 7. No. 1, (2006).

[58] V. M. Garcia, M.T. Nair P.K. Nair and Zingaro, "*Preparation of highly photosensitive CdSe thin films by CBD",* **Semiconductor Science and Technology, 3**,March (1996) .p. 427-423.

[59] P. Nemec, D. Mikes, J. Rohovec, E. Uhlirova, F. Trojanek, P. Maly. *"L:ight –controlled growth of CdSe NC films prepared by CBD"* , **Material Science and Engineering,** p. 69-70 (2000) 500-504.

[60] C. Mehta, J. M. Abbas, G. S. Saini, S. K. Tripathi. "*Effect of deposition parameters on the optical and electrical properties of nanocrystalline CdSe thin films"*. **Chalcogenides Letters** Vol. 4, (2007), p. 133-138.

[61] S. S. Kale and C. D. Lokhande, "*Thickness-dependent properties of chemically deposited CdSe thin films"*. **Materials Chemistry and Physics,** V. 62,(2000), p.103-108.

[62] P. P. Hankare, S. D. Delekar, Asabe, P. A. Chate, Bhuse, A. S. Khmane, K. M. Garadkar and B. D. Sarwade. *"Synthesis of CdSe thin films at low-temp. by simple Chemical route and their Characterization",* **Journal of Physics and Chemistry of Solids,** V.67, (2006), p. 2506-2511.

[63] S. Erat and H. Metin, "*Structural and Optical Properties of CdSe Films Prepared by CBD",* **AIP Conf. Proc.** V. 899, (2007), p. 249-250.

[64] M. S. Sung, Y. B. Lee, Y. S. Kim, y. Rhyim, J. C. Kim, I. B. Kim, Y. D. Kim, "*Preparation and Characterization of CdSe Nanoparticles, Ultrasonic Irradiation",* **Journal of Nano Research, ICCST**/7: 7th International Conference, (2009).

[65] P. Nemec, M. Simurda, I. Nemec, D. Spinzl, D. Fomanek and P. Maly." *Highly luminescent CdSe nanocrystalline films prepared by chemical bath deposition".* **Journal of Crystal Growth,** V.292, (2006), p. 78-86.

[66] See ref. [62] p. 2511.

[67] R. B. Kale, C. D. Lokhande," *Influence of air annealing on the structural, optical and electrical properties of chemically deposited CdSe nanocrystallites",* **Applied Surface Science**, 223 (2004), p. 343-351.

[68] H. S. Hilal, C. Kim and A. F. Schreiner, "*Preparation and Characterization of Tetra(-4-pyridyl) porphyrinatomanganese Cation Supported Covalently on Poly(siloxane)",* J. Mol. Catal, 64 (1991) 133; *"Preparation and Characterization of Poly(siloxane)-Supported Metalloporphyrine: The Effect of the Support on the Electronic Absorption Spectra",* **Inorg. Chem. Acta**, 189 (1991) L141.

[69] N. Kobayashi, H. Seiki, T. Osa, "*Catalytic Electro reduction of Molecular Oxygen using [5, 10, 15, 20-tetrakis-(1-methylpyridinium-4-yl) porphinato] manganese",* **Chem. Lett**. (1985) 1917.

[70] M. M. Masoud, "*Surface Modification of n-GaAs Semiconductor with Metalloporphyrine/Polysiloxane Matrices, Effect of Modification on: Band –Edge Position, Short Circuit Current and Surface Stability in Aqueous photoelectrochemstry"* **(Unpublished master's thesis). An-Najah National University**, Nablus, Palestine, (2001) p. 34.

[71] See ref. [70] p. 35.

[72] See ref. [70] p. 35.

[73] See ref. [70] p. 36.

[74] See ref. [70] p.36.

[75] R. Tenne, G. Hodes, "*Improved Efficiency of CdSe Photo anodes by PEC Etching"*, **App. Phys. Lett**., 37 (1980) p. 420-430.

[76] See ref. [67] p. 344.

[77] B. Pejova and I. Grozdanov, "*Manifestation of three dimensional confinement in the optical spectra of CdSe quantum dots in thin film form",* **Material Letters** V. 58, (2004) , p. 666-671.

[78] See ref. [70] p. 46.

[79] See ref. [67] p. 347.

[80] H.S. Hilal, S.K. Salih, I.A. Saadeddin, G. Campet, *"Effect of cooling rate on n-GaAs electrode photoelectrochemical characteristics",* **Act. Pass. Electron. Comp.** 25 (2003) p. 1-12.

[81] H.S. Hilal, M. Masoud, S. Shakhshir, N. Jisrawi, J. Electroanal."*Surface Modification of n-GaAs SC with MnP/polysiloxane Matrices, Effect of Modification on :Band Edge Position, Short Circuit Current and Surface Stability in Aqueous PEC"*
Chem. 527 (2002) p. 47–55.

[82] H.S. Hilal, M. Masoud, S. Shakhshir, N. Jisrawi," *Surface modification of n-GaAs semiconductor with metalloporphyrine/polysiloxane matrices effect of modification on band-edge position, short circuit current and surface stability in aqueous photoelectrochemstry",* **Act. Pass. Electron. Comp**. 26 (2003) 11–21.

[83] See ref. [67] p. 345.

[84] S. H. Jeedigunta, P. Spagnol, J. Bumgarner, A. Kumar, *"Electrical contacts to nitrogen incorporated nanocrystalline diamond films"* , **Diamond and Related Materials**, V. 17, (2004), p. 39.

[85] See ref. [59] p. 503.

[86] See ref. [60] p. 137.

[87] See ref. [61] p. 105.

[88] C. D. Lokhande, "*Electrosynthesis of CdSe Films on Nickel substrate"*, **Institute of science and technology**, P.O. box 131, Republic of Korea, (2004).

[89] C. M. Shen, X. G. Zhang and H. L. Li" *Influence of different deposition potentials on morphology and structure of CdSe films*", **Applied Surface Science,** V.240, (2005), p. 34-41.

[90] R. A. Boudreau and R. D. Rauh," *CBD of thin film CdSe for PEC cells"*, **Electrochemical Society, Journal**, V. 130, (1983), p. 513-516.

[91] D. P. Padiyan, A. Marikani and K. R. Murali," *Influence of thickness and substrate temperature on electrical and photoelectrical properties of vacuum-deposited CdSe thin films"*, **Materials Chemistry and Physics,** V. 78, (2003), p. 51-58.

[92] S. K. Sharma, L. Kumar, S. Kumar, T. P. Sharma, "*Dependence of band gap on deposition parameters in CdSe sintered films",* **Chalcogenide Letters** V. 5, (2008), p. 73-78.

[93] G. Hodes, A. Albu-Yaran, F. Decher, P. Matsuke, "*Influence of Light Illumination During Chemical Deposition of CdSe NC'S*", **Phys. Rev.** , p. 36, (1987) 4215.

[94] See ref. [67] p. 348.

[95] See ref. [62] p. 2509.
[96] See ref. [63] p. 249-250.
[97] See ref. [62] p. 2510.
[98] See ref. [63] p. 249-250.
[99] See ref. [80] p.46.
[100] See ref. [81] p.51.
[101] D. Y. Chae, K. W. Seo, S. S. Lee, S. H. Yoon and I. W. Shim, "*ZnSe thin films grown by MOCVD method using new single-source precursors",* **Bull Korean Chem. Soc**. V. 27, (2006), p. 762-764.

[102] F. I. Ezema, R. U. Osuji, "*Band gap shift and optical characterization of CBD CdSSe thin on annealing, "***Chalcogenide Letters**, V. 4, (2007), p. 69-75.

[103] E. U. Masumdar, L.P. Deshmukh, "*Photoelectrochemical properties of CdSe:Sb thin film based solar cell, influence of electrode thickness",* **J. Phys.** (2003), p. 271-278.
[104] S. Claesson, B. Holmstrom, "*Solar Energy Photochemical Processes*

Available for Energy Conversion", Swedish, (1983), p. 200–210.
[105] V.D. Das, J. Sathyanarayanan, L. Damodare, "*Enhancement* of *n-GaAs characteristics",* **Surf. Coat. Technol**. 94–95 (1997) 669–671.

[106] See ref. [82].p. 11-23.
[107] See ref. 80, p. 55.

[108] R. Singh, M. Fakhruddin, K.F. Poole, "*Rapid thermal processing s semiconductor manufacturing for the 21st century",* **Appl. Surf. Sci.** 168 (2000) 198–203.

[109] A. Claverie, B. Colombeau, G.B. Assayag, C. Bonafos, F. Cristiano,

B. Mauduit, "*Epitaxial growth of semiconductors on $SrTiO_3$ substrates*", **Mater. Sci. Semicond. Proc. 3** (2000) 269–277.
[110] See ref. [105], p. 669–671.
[111] H. Fujioka, J. Ohta, H. Katada, T. Ikida, Y. Noguchi, M. Oshima, " *Enhancement of n-GaAs characteristics* by combined heating, *cooling rate and metalloporphyrine modification techniques*", **J. Cryst. Growth 229** (2001) 137–141.

[112] A. Ndiaye and I. Youm, "*Effect of post-deposition processing on micro structural thin films grown from solution",* **Eur. Phy. J.** (2003), p. 75-82.
[113] Y. Nishijima, K. Makajima, K. Ostubo, H. Ishikama, *"InGaAs single crystal with a uniform composition the growth direction grown on InGaAs seed using the multicomponent zone growth method",* **J. Cryst. Growth** 208 (2000) 171–178.
[114] U. Pal, S. Munoz, L. Pardo, R. Silva, J.M. Gracia, "*Effect of laser annealing on the distribution of defect levels in CdSe films"***, Thin Solid Films,** V. 381, (2001), p. 155-159.
[115] See ref. [80] p. 38.
[116] See ref. [81] p. 54.
[117] H.O. Finklea, in H.O. Finklea (Ed.)," *Semiconductor Electrodes*", **Elsevier, Amsterdam,** (1988), p. 373.
[118] See ref. [67] p. 348.
[119] See ref.[67] p. 348.

تحسين خواص أفلام سلينيد الكادميوم الرقيقة في خلايا تحويل الضوئي الكهربائي

إعداد

هدى سليمان محمد صبري

إشراف

د. صبحي كامل صالح

أ.د. حكمت سعيد هلال

ملخص

تم ولأول مرة تحضير أفلام CdSe على شرائح زجاجية مغطاة بطبقة رقيقة موصلة شفافة من أكسيد القصدير المزود بالفلور (FTO) بطريقة الترسيب الكيميائي (CBD). تم ترسيب الأفلام باستخدام كلوريد الكادميوم كمصدر لأيونات الكادميوم، وسلينيوكبريتيد الصوديوم كمصدر لأيونات السلينيد السالبة. وبعد تحضيرها وتسخينها لدرجات حرارة مختلفة (١٠٠°م، ١٥٠°م، ٢٠٠°م، ٢٥٠°م، ٣٠٠°م و ٣٥٠°م)، لوحظ أن التسخين يؤدي الى تأثيرات مختلفة على خصائص الأفلام ، مثل الصفات المطيافية الامتصاصية و الانبعاثية و مقدار فجوة الحزمة (E_g Band gap).نظرا لعدم ثباتية الأفلام المحضرة، لم نتمكن من دراسة خصائصها الفوتوكهروكيماوية، حيث أعطت منحنيات شدة تيار مع الجهد غير متناسبة مع أشباه الموصلات، حيث لوحظ أن سبب ذلك هو تقشر طبقة الفلم عن الشرائح. وفي محاولة منا لتحسين ثباتية الأفلام في ظروف فوتوكهروكيماوية، تم حك طبقة FTO قبل ترسيب الفلم عليها، وقد حسن ذلك من صفات الفلم جزئيا فقط. ومن أجل تحسين ثباتية و صفات الأفلام في ظروف فوتوكهروكيماوية، تم طلاؤها بطبقة من مركبات بورفرينات المنغنيز مع مبلمر عديد السايلوكسين. وتتبع هذه الطريقة هنا لأول مرة في أفلام CdSe وأعطت نتائج مشجعة. لوحظ أنه يمكن الوصول لأفضل النتائج من خلال استخدام التسخين و التبريد المسبق للأفلام ثم طليها بطبقة من البورفرينات مع بولي سايلوكسين. في هذه الرسالة نعرض النتائج المتعلقة باستخدام الأفلام في عمليات تحويل الطاقة الضوئية الى طاقة كهربائية.

جامعة النجاح الوطنية

كلية الدراسات العليا

تحسين خواص أفلام سلينيد الكاديوم الرقيقة في خلايا تحويل الضوئي الكهربائي

إعداد

هدى سليمان محمد صبري

إشراف

د. صبحي كامل صالح

أ.د. حكمت سعيد هلال

قدمت هذه الأطروحة استكمالا لمتطلبات درجة الماجستير في الفيزياء بكلية الدراسات العليا في جامعة النجاح الوطنية في نابلس، فلسطين.

2009